Università degli Studi di Padova

Dipartimento di Matematica Tullio Levi Civita

Courso di Laurea in Matematica

Titolo da decidere

Relatrice:
Prof. Callegaro Giorgia

Candidato:
Hu Nicola
Numero di matricola:
1217174

Academic Year 2020/2021

Contents

Notation

- $\mathbb{C}$ are the complex numbers.

- $\mathbb{R}_+$ are the positive real numbers.

- $C^\alpha(\mathbb{R})$, for $\alpha \in (0,1]$, denotes the space of α-Hölder continuous functions, defined below in Definiton 4.

- $AC([a,b])$ is the space of absolute continuous functions on $[a,b]$, where $-\infty \le a < b \le +\infty$. We remind that f is absolutely continuous in $[a,b]$ if for any $\epsilon > 0$, there exists $\delta > 0$ s.t. for any finite set of n disjoint intervals $[a_k, b_k]$ contained in $[a,b]$ satisfying $\sum_{k=1}^n (b_k - a_k) < \delta$, we have $\sum_{k=1}^n |f(a_k) - f(b_k)| < \epsilon$.

- $AC^n([a,b])$, for n positive integer and $-\infty \le a < b \le \infty$, is the space of functions f with continuous derivatives up to the order $(n-1)$ on (a,b) and with $f^{(n-1)} \in AC([a,b])$.

- $\lfloor x \rfloor$ for $x \in \mathbb{R}$, denotes the largest integer smaller than x.

- $\lceil x \rceil$ for $x \in \mathbb{R}$, denotes the smallest integer greather than x.

- $\{x\}$ for $x \in \mathbb{R}$ is the fractional part of x, i.e. $\{x\} = x - \lfloor x \rfloor$.

- $\Gamma(x) = \int_0^{+\infty} s^{x-1} e^{-s}\, ds$, with $x > 0$ is the Gamma function.

- $B(x,y) = \int_0^1 s^{x-1}(1-s)^{y-1}\, ds$, with $x, y > 0$ is the Beta function.

Introduction

The classical Heston model is the most famous stochastic volatility model describing the dynamics of S, the underlying asset price, and V, the variance process. It consists of the following stochastic differential equations:

Classical Heston model.

$$\begin{cases} dS_t = S_t\sqrt{V_t}dW_t, \\ dV_t = \eta(m - V_t)dt + \eta\zeta\sqrt{V_t}dB_t, \\ S_0 = s_0 > 0, \\ V_0 = v_0 > 0, \\ t \geq 0, \end{cases} \tag{1}$$

where W and B are two Brownian motions with correlation ρ (i.e., $Corr(dW_t, dB_t) = \frac{Cov(dW_t, dB_t)}{\sqrt{Var(dW_t)}\sqrt{Var(dB_t)}} = \rho dt$).
In this model the volatility follows a standard Brownian motion.

Despite its celebrity, it has been shown that this model does not represent accurately historical volatility time-series, as these happen to be rougher than what this model allows (i.e., a standard Brownian motion). A "roughening" of this version has been elaborated. This has been inspired by (see [12]) the fractional Brownian motion (which is a generalization of the Brownian motion and allows for a rougher behaviour).

A fractional Brownian motion $(W_t^H)_{t \geq 0}$ with Hurst index $H \in (0, 1)$ can be expressed with the Mandelbrot-Van Ness integral representation (as we will see in more details later in subsection 1.1.2):

$$W_t^H = \frac{1}{\Gamma(H + \frac{1}{2})}\int_{-\infty}^0 [(t-s)^{H-\frac{1}{2}} - (-s)^{H-\frac{1}{2}}]dZ_s + \frac{1}{\Gamma(H + \frac{1}{2})}\int_0^t (t-s)^{H-\frac{1}{2}}dZ_s, \tag{2}$$

where $(Z_s)_{s \geq 0}$ is a standard Brownian motion and $t \geq 0$.

The regularity of the trajectories of a fractional Brownian motion are determined by its kernel $(t-s)^{H-\frac{1}{2}}$. In particular we will show that the term:

$$\int_0^t (t-s)^{H-\frac{1}{2}} dZ_s, \qquad t \in \mathbb{R}_+ \tag{3}$$

has Hölder regularity of at most H (H excluded), namely it has α-Hölder regularity (see Definition 4 below) for any $\alpha \in (0, H)$ and is not α-Hölder regular for any $\alpha \geq H$. Moreover, the term (3), shares the same regularity properties of (2), as we will show later. In particular, the fractional Brownian motion W^H of Hurst index H is rougher when H is small. The case $H < \frac{1}{2}$ models a rough behaviour (i.e., paths are less smooth).

Therefore, inspired from the fractional Brownian motion, if we want to introduce some rough behaviour in the Heston model, it becomes natural to introduce the kernel $(t-s)^{\alpha-1}$ in the classical Heston model, where $\alpha = H + \frac{1}{2}$, obtaining the:
Rough (or fractional)[1] Heston model:

$$\begin{cases} dS_t = S_t \sqrt{V_t} dW_t, \\ V_t = V_0 + \frac{1}{\Gamma(\alpha)} \left(\int_0^t (t-s)^{\alpha-1} \eta(m - V_s) ds + \int_0^t (t-s)^{\alpha-1} \eta\zeta\sqrt{V_s} dB_s \right), \\ S_0 = s_0 \in \mathbb{R}_+, \\ V_0 = v_0 \in \mathbb{R}_+, \end{cases}$$
$$\tag{4}$$

where ζ, η, $m \in \mathbb{R}_+$, and W, B are two Brownian motions with correlation ρ, in analogy with W and B in the classical Heston model (1).

Notice the differences with the classical Heston model (1). The Variance differential equation here is an integral equation. In the differential Variance equation of (1) we introduced the kernel $(t-s)^{\alpha-1}$ ($\alpha \in (0,2)$), multiplied by a constant (namely, $\frac{1}{\Gamma(\alpha)}$) and then integrated. These are not random operations: we attempted to reproduce the Mandelbrot-Van Ness integral representation of a stochastic fractional Brownian motion, as we want to allow for rougher behaviours than this stochastic process allows to. Notice that we only reproduced the kernel term of the Mandelbrot-Van Ness integral representation, as this controls the regularity (or rough behaviour) of the trajectories. Finally, observe that (4) is a generalization of (1), as for $\alpha = 1$, the system of equations (4) is exactly (1).

The corresponding integral equation of a differential equation exists under appropriate integrability conditions, and in this case these are equivalent.

---

[1] We take inspiration from the "fractional" Brownian motion.

So far we discussed about the standard Brownian motion, the Heston model, and their respective fractional versions. There is another key ingredient we need: the Riccati differential equations (and their fractional version).

As showed in [11] and [3], for the classical Heston model (1), there exists an explicit formula for the characteristic function of the log-price $X_t := \log(\frac{S_t}{S_0})$, and this is:

$$E[e^{u_1 X_t}] = \exp[\phi_1(t) + \phi_2(t)V_0] \tag{5}$$

where $\phi_1(t)$ is a solution to the Riccati differential equation:

$$\partial_t \phi_1 = \frac{1}{2}(u_1^2 - u_1) + \eta(u_1 \rho \zeta - 1)\phi_1(s) + \frac{(\eta\zeta)^2}{2}\phi_1^2(s), \quad \phi_1(0) = 0 \tag{6}$$

where $u_1 \in i\mathbb{R}$, $t > 0$, and ϕ_2 satisfies:

$$\phi_2(t) = \eta m \int_0^t \phi_1(s)\,ds. \tag{7}$$

This summarises as: the classical Heston model (1) has a closed formula (5) for $X_t := \log(\frac{S_t}{S_0})$ (S_t solving the classical Heston model (1)), which is resolved through a Riccati differential equation (6).

As for the fractional Heston model (see [3] for proof), there is also an explicit formula for the characteristic function of the log-price $X_t := \log(\frac{S_t}{S_0})$ (S_t solving the fractional version (4), not the classical (1)), and this is:

$$E[e^{u_1 X_t}] = \exp[\phi_1(t) + \phi_2(t)V_0] \tag{8}$$

where $u_1 \in i\mathbb{R}$, $t > 0$ and

$$\begin{cases} \phi_1(t) = m\eta \int_0^t \psi(s)\,ds \\ \phi_2(t) = I_{1-\alpha}\psi(t) \end{cases} \tag{9}$$

where ψ solves the fractional differential Riccati equation

$$D^\alpha \psi(t) = \frac{1}{2}(u_1^2 - u_1) + \eta(u_1 \rho \zeta - 1)\psi_1(t) + \frac{(\eta\zeta)^2}{2}\psi_1^2(t), \quad I_{1-\alpha}\psi(0) = 0, \tag{10}$$

where D^α and $I_{1-\alpha}$, are fractional Riemann-Liouville integrals and derivatives. We remind that we introduced the coefficient $\alpha \in (0,2)$ in the passage from the classical Heston model to the fractional Heston model (4). For the existence and uniqueness of a solution to this Riccadi differential equation we refer to [3].

Notice that with the fractional differential Riccati equation we substituted the regular differentiation with the fractional Riemann-Liouville differentiation, which will be defined rigorously later in Definition 7.

Now we can wrap up: the classical Heston model (1), whose volatility is driven by a standard Brownian process, has a formula for the characteristic function of the log-price (5). This is resolved through a differential Riccati equation (6). By introducing the fractional Heston model (4), whose volatility is driven by a fractional Brownian motion process, the relationship with the previous Riccati differential equation is not lost. This is preserved, but the Riccati differential equation becomes now a fractional Riccati differential equation (11).

Our main aim is to solve the fractional Riccadi ODE with constant coefficients (we use the same notation as [5]):

$$[\mathcal{E}^{u,v}_{\lambda,\mu,\nu}] \equiv D^\alpha \psi = \lambda \psi^2 + \mu \psi + \nu, \begin{cases} I_{1-\alpha}\psi(0) = u \in \mathbb{C}, & \text{if } \alpha \in (0,1], \\ I_{1-\alpha}\psi(0) = u, I_{2-\alpha} = v, & \text{if } \alpha \in (1,2], \end{cases} \tag{11}$$

where $\lambda, \mu, \nu, u, v \in \mathbb{C}$.

Notice that for $\alpha \in (0,1]$ we have one initial condition, while for $\alpha \in (1,2]$ we have two initial conditions. In order to grant uniqueness to a general ODE of order $n \in \mathbb{N}$, we have n initial conditions. For the fractional differential equations of order $\alpha \in \mathbb{R}_+$, we grant $\lceil \alpha \rceil$ initial conditions.

Note that in order to compute the characteristic function for the log-price we just need to solve fractional Riccati ODE with null initial conditions.

remark. Probably we will be only solving the null initial conditions, as this thesis is already long. And $\alpha \in (0,1)$, as it is similar the procedure for $\alpha \in (1,2)$. However I can say something about the not null initial conditions as discussed in the paper.
NOT FINISHED YET. THIS last part of the introduction to finish later.
In this work we will solve the null initial condition case. For the non null initial condition see paper.
We will solve only for $\alpha \in (0,1]$. However, the case $\alpha \in (1,2]$ has analogous procedure, both for fractional Riccati and for Euler scheme.
Our approach: To Add Later on ... 1) first transform the differential into integral equation

2) Then discuss a bit of fractional power series centered in 0.
The idea is to express the solution of the fractional Riccati as fractional power series. ... Talk about some steps about the convergence radius finite,

numerical etc...

Talk about the estimate of the error.

Also have to change the Mandelbrot. The name I wrote is spelled wrongly.

3) Our approach etc.. etc.. and end.

Chapter 1

Preliminaries

1.1 Fractional Brownian Motion

The fractional Brownian motion (henceforth fBm) is a stochastic process denoted by W^H, $H \in (0,1)$ is a constant called the "Hurst Index".
The name *fractional Brownian motion* was introduced by Mandelbrot and Van Ness in 1968, who provided a stochastic integral representation in terms of a Brownian motion.

Before giving the definition, we recall the following:

Definition 1 (Gaussian Process)**.**
A time continuous stochastic process $\{X_t | t \in T\}$ is Gaussian if for every finite subset of times $t_1, \cdots, t_k \in T$, we have that the random vector

$$(X_{t_1}, \cdots, X_{t_k})$$

is a multivariate Gaussian, i.e. every linear combination of $X_{t_1}, \cdots, X_{t_k}$ has Gaussian distribution. Moreover we say that the Gaussian process is centered if X_t has mean 0 for all $t \in T$.

Now we define the Fractional Brownian Motion:

Definition 2 (Fractional Brownian Motion (Ref. [2], Part I, section 1.1))**.**
Let $H \in (0,1)$ a constant. A fractional Brownan motion $(W_t^H)_{t \geq 0}$ of Hurst index H, is a continuous centered Gaussian process with covariance function:

$$C(t,s) := Cov[W_t^H, W_s^H] = \frac{1}{2}(t^{2H} + s^{2H} - |t-s|^{2H}), \qquad s, t \geq 0. \quad (1.1)$$

This is a good definition: it does indeed exist a unique centered Gaussian process, whose covariance function satisfies equation (1.1).
The existence of a Gaussian process with covariance (1.1) is granted by the

general existence theorem for centered Gaussian processes with a given covariance function (see [1], Part I, section 1.1). Moreover it is unique in the sense that, given $(X_t)_{t\geq 0}$ and $(Y_t)_{t\geq 0}$ two Gaussian processes with the same mean and covariance functions, then X and Y are identical in law (see [6], Section 1.).

Therefore the definition of fBm is consistent.

Note that for the covariance function we have the following identity:

$$C(t,s) = E[W_t^H W_s^H] - E[W_t^H]E[W_s^H] = E[W_t^H W_s^H] \qquad (1.2)$$

since $E[W_t^H] = 0$ for any $t \geq 0$, as W^H is a centered Gaussian.

1.1.1 Main Basic Properties of the fractional Brownian motion

A fractional Brownian motion has the following basic properties (from [2], Part I, section 1.1):

Proposition 1. *Let $(W_t^H)_{t\geq 0}$ be a fractional Brownian motion. Then:*
- *$W_0^H = 0$ a.s. and $E[W_t^H] = 0$ for all $t \geq 0$.*
- *W_t^H has stationary increments: the law of $\left(W_{t+s}^H - W_t^H\right)$ is the same as the law of W_t^H, for all $s, t \geq 0$.*
- *W_t^H has continuous trajectories [1].*

Proof.
The first property is immediate: use the covariance equation (1.1) from the Definition 2 of fractional Brownian motion with $t = s = 0$. The expected value of the square is zero, and then $W_0^H = 0$ a.s.
The expectation $E[W_t^H] = 0$ for all $t \geq 0$ is a direct consequence of the fact that W_t^H is a centered Gaussian process.
For the second property, use the fact that two Gaussian processes are equal in law if and only if they have same mean and same autocovariance function (see [9] Lemma 11.1). The mean is zero for both. The autocovariance function is also the same after computations and using property (1.1). Hence they have the same law.
The third property is a direct consequence of Theorem 1 (Regularity of Sample Paths of fBm), which will be discussed later.

∎

Remark 1. *The fractional Brownian motion is classified into 3 special classes depending on the values of H: $0 < H < \frac{1}{2}$, $H = \frac{1}{2}$ and $\frac{1}{2} < H < 1$. In particular, when $H = \frac{1}{2}$, the fractional Brownian motion $W^{\frac{1}{2}}$ coincides with the usual standard Brownian motion.*

---

[1]Note that a centered Gaussian process may not have continuous trajectories. See Example 2.1 in [6].

1.1.2 Stochastic Integral Representation: Mandelbrot-van Ness representation.

There are several different integral representations of the fractional Brownian motion (see [8], chapter 2, section 2.3). We will discuss the

Mandelbrot-van Ness representation:

$$Z_t = \frac{1}{\Gamma(H + \frac{1}{2})} \int_{-\infty}^{0} ((t-s)^{H-\frac{1}{2}} - (-s)^{H-\frac{1}{2}}) dW_s + \frac{1}{\Gamma(H + \frac{1}{2})} \int_{0}^{t} (t-s)^{H-\frac{1}{2}} dW_s,$$
(1.3)

for any $t \geq 0$ and $(W_s)_{s \geq 0}$ is a standard Brownian motion.
It can be proved that the process Z_t (see [7]) is a centered Gaussian process, whose covariance function is given by equation (1.1). Hence $Z_t = W_t^H$ is the fractional Brownian motion of Hurst index $H \in (0, 1)$.

We refer to $(t - s)^{H-\frac{1}{2}}$ as the kernel of the fractional Brownian motion. This determines the regularity of the trajectories of the fBm (as we will discuss later in equation (1.14)).

Another important property is the so called long-short memory of the fractional Brownian motion.

1.1.3 Long and Short Memory of the fractional Brownian motion.

One main fact is that, while for $H = \frac{1}{2}$ the increments of W_t^H are independent [2], increments for $H \neq \frac{1}{2}$ are not (see [2], Part I, section 1.3). More precisely,

Remark 2. *The correlation between* $\left(W_{t+h}^H - W_t^H\right)$ *and* $\left(W_{s+h}^H - W_s^H\right)$ *is not zero if* $H \neq \frac{1}{2}$. *It is positive if* $\frac{1}{2} < H < 1$, *and negative if* $0 < H < \frac{1}{2}$.

Proof. Let $t = s + nh$ for $t, s, h \geq 0$ and $n \geq 1$ integer.
The covariance between $\left(W_{t+h}^H - W_t^H\right)$ and $\left(W_{s+h}^H - W_s^H\right)$ is

$$
\begin{aligned}
Cov[\left(W_{t+h}^H - W_t^H\right), \left(W_{s+h}^H - W_s^H\right)] = \\
E[(W_{t+h}^H - W_t^H)(W_{s+h}^H - W_s^H)] = \\
\frac{1}{2} \left(-2(t-s)^{2H} + (t-s-h)^{2H} + (t+h-s)^{2H}\right) = \\
\frac{1}{2} \left(-2(nh)^{2H} + (h(n+1))^{2H} + (h(n-1))^{2H}\right) = \\
\frac{1}{2} h^{2H} \left(-2n^{2H} + (n+1)^{2H} + (n-1)^{2H}\right) =: \rho_H(n),
\end{aligned}
$$
(1.4)

---

[2]This is a well-known property of the standard Brownian motion.

where we used the linearity of the expected value and the property (1.1) of
a fractional Brownian motion.

From this we can deduce that for $H = \frac{1}{2}$, the correlation between increments
is zero, i.e. increments are independent, which is a known property of the
standard Brownian motion.

Finally, it is easy to see that for $H > \frac{1}{2}$ we have positive covariance and this
case includes the long memory property of the fBm that we will see below in
Lemma 1. While for $H < \frac{1}{2}$ the covariance is negative and this case includes
the short memory property of the fBm.

<div style="text-align:right">■</div>

From this proof we observe that the covariance between increments de-
pends uniquely on the value of the increment h and the distance between
the times s and t $(t - s = nh)$, while it does not depend on the individual
values of s and t.

One important thing about fractional Brownian motions is that, for
$H > \frac{1}{2}$, the process W_t^H has long memory, while for $H < \frac{1}{2}$ there is a short
memory.

Lemma 1. *The followings hold:*
For $H > \frac{1}{2}$,

$$\sum_{n=1}^{\infty} \rho_H(n) = \infty \tag{1.5}$$

while for $H < \frac{1}{2}$

$$\sum_{n=1}^{\infty} |\rho_H(n)| < \infty. \tag{1.6}$$

The first (1.5) is called long memory (or long range dependence) of the
fBm. The latter (1.6) is the short memory behavior (or short range depen-
dence). This is an important fact: it states that the fractional Brownian
motion W^H, for $H > \frac{1}{2}$, has a range of dependency from the past long
enough to make the series of correlations $(\rho_H(n))_{n \in N}$ diverge. On the other
hand, for $H < \frac{1}{2}$, the range of dependency from the past is shorter.

According to Definition 1.4.1 in [2]:

Definition 3. *A sequence $(X_n)_{n \in \mathbb{N}}$ exhibits long-range dependence if $\rho(n) :=$*
$cov(X_{k+n}, X_k)$ satisfies:

$$\lim_{n \to \infty} \frac{\rho(n)}{n^{-\alpha}} = c \tag{1.7}$$

for some positive constant c and $\alpha \in (0, 1)$.

In this case, the dependence between X_{k+n} and X_k decays slowly as n increases. Moreover, if (1.7) holds, then we have:

$$\sum_{n=1}^{\infty} \rho(n) = \infty. \tag{1.8}$$

Let us prove Lemma 1

Proof. of Lemma 1

Lemma 1 easily follows from:

$$\rho_H(n) = \frac{1}{2} h^{2H}((n+1)^{2H} + (n-1)^{2H} - 2n^{2H}) \sim n^{2H-2} \tag{1.9}$$

as $n \to \infty$. This is easy to verify. Dividing the LHS by the RHS, we can then use the Taylor expansion for the binomial and the result follows.

From (1.9), we clearly see that the series

$$\sum_{n=1}^{\infty} \rho_H(n) \sim \sum_{n=1}^{\infty} n^{2H-2} =: \zeta(2H - 2), \tag{1.10}$$

where we informally used the asymptotic symbol to denote that the n-th term of the first series is asymptotic to the n-th term of the second series, as $n \to +\infty$.

The RHS is the known Riemann series. This converges for $H < \frac{1}{2}$ and diverges for $H > \frac{1}{2}$, as desired. ∎

The last property of the fractional Brownian motion W^H that we will discuss is about the regularity of the trajectories. We will see that this depends on the value of the Hurst index H.

1.1.4 Path Regularity and Rough behaviour of the fractional Brownian motion.

The paths of a fractional Brownian process $(W_t^H)_{t \geq 0}$ are at most H-Hölder continuous. More precisely,

Theorem 1 (Regularity of Sample Paths of fBm)**.** *The sample paths of a fractional Brownian motion W^H are α-Hölder continuous for any $\alpha \in (0, H)$. Moreover, it is not H-Hölder continous.*

First let us recall:

Definition 4 (Hölder continuity)**.** *A function $f : \mathbb{R} \to \mathbb{R}$ is Hölder continuous of order α (or simply α-Hölder continuous), with $0 < \alpha \leq 1$, if there exists $M > 0$ such that*

$$|f(y) - f(x)| \leq M|x - y|^{\alpha} \tag{1.11}$$

for any $x, y \in \mathbb{R}$ (or in a compact domain, in which case we would restrict the Hölder continuity to the domain). In this case, we denote it as $f \in C^{\alpha}(\mathbb{R})$.

We recall some properties of α-Hölder continuous functions:
• An α-Hölder continuous function with $\alpha \in (0, 1]$ is uniformly continuous. Hence it is also continuous.
• If $f \in C^{\alpha}(\mathbb{R})$, then also $f \in C^{\beta}(\mathbb{R})$ for any $\beta \in (0, \alpha]$.

Remark 3. *The first property tells us that sample paths of a fractional Brownian motion are continuous.*

Now let us prove Theorem 1 (Regularity of Sample Paths of fBm, ref. [8], Proposition 1.6).

Proof.
Recall the Kolmogorov criterion (ref. [2], Part I, section 1.6): let $X = (X_t)_{t \in \mathbb{R}}$ be a Gaussian process. Suppose that there exist constants $\beta > 0$ and $k > 0$ such that

$$E[|X_t - X_s|^2] \leq k(t - s)^{\beta} \tag{1.12}$$

for all $t, s \in \mathbb{R}$. Then X admits a continuous modification Y, whose paths are α-Hölder continuous for all $\alpha \in (0, \frac{\beta}{2})$.

Let us verify (1.12) for W^H:

$$E[(W_t^H - W_s^H)^2] = |t - s|^{2H}, \tag{1.13}$$

where the equality follows by the linearity of the expected value and by applying the covariance property (1.1) of the fBm. Therefore the criterion is satisfied with $\beta = 2H$, and W^H admits a continuous modification, whose paths are at most $\beta/2 = H$-Hölder continuous.
Hence, the $\alpha-$Hölder continuity of the sample paths, for $\alpha \in (0, H)$ holds. The fact that the sample paths are not $H-$Hölder continuous is omitted (see [8], Proposition 1.6 for proof.).

∎

Now one final note about the Mandelbrot and Van Ness integral representation and the α-Hölder continuity.
We remind that the fractional Brownian motion W_t^H can be expressed with the following:

$$W_t^H = \frac{1}{\Gamma(H + \frac{1}{2})} \int_{-\infty}^{0} ((t-s)^{H-\frac{1}{2}} - (-s)^{H-\frac{1}{2}}) dW_s + \frac{1}{\Gamma(H + \frac{1}{2})} \int_{0}^{t} (t-s)^{H-\frac{1}{2}} dW_s.$$
(1.14)

This representation is the sum of two terms. The latter is the one with the kernel $(t-s)^{H-\frac{1}{2}}$, and this has the same regularity properties of the paths of W^H. Indeed, we see that the first term of the Mandelbrot-Van Ness representation is even differentiable (differentiation under integral sign), while the trajectories of W^H are not differentiable (see [2]). Therefore it follows that the α-Hölder continuity property of the paths of W^H transmits to the second term, the one containing the kernel. Hence, as we briefly anticipated in the introduction, the regularity of the paths of a fractional Brownian motion W^H, are transferred to the term containing the kernel in the Mandelbrot-Van Ness representation and viceversa (it cannot be that one is more regular than the other). This is why in the literature you may come across the expression "the kernel determines the regularity of the paths of the fractional Brownian motion".

To conclude, let us see some plots (Figure 1.1) of fractional Brownian motion's paths. We generate them randomly with Python (see Appendix for the source code. The exeeriments are run on a computer with 12 CPUs i7-8750H @ 2.20GHz). We use the open-source library "fbm" from Christopher Flynn.

(a) H=0.2

(b) H=0.4
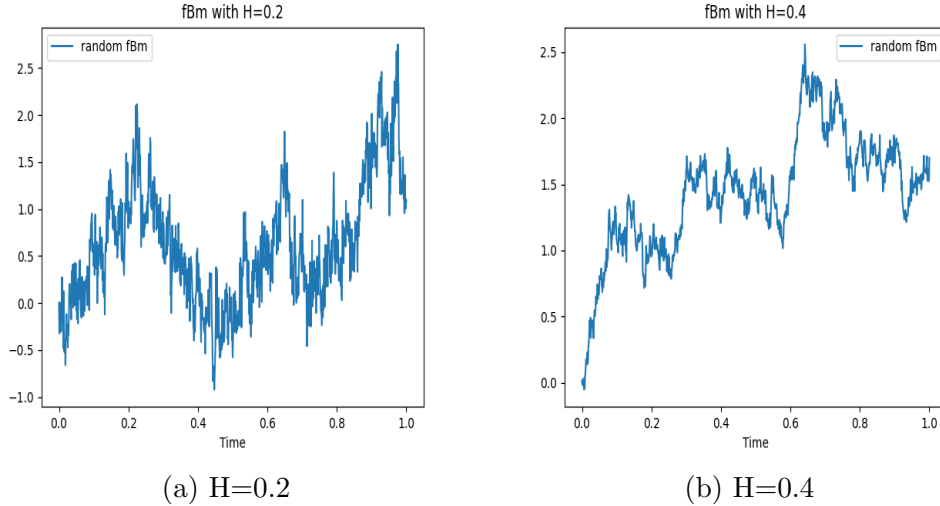
As we can see from the plots, the sample paths of W^H are at most
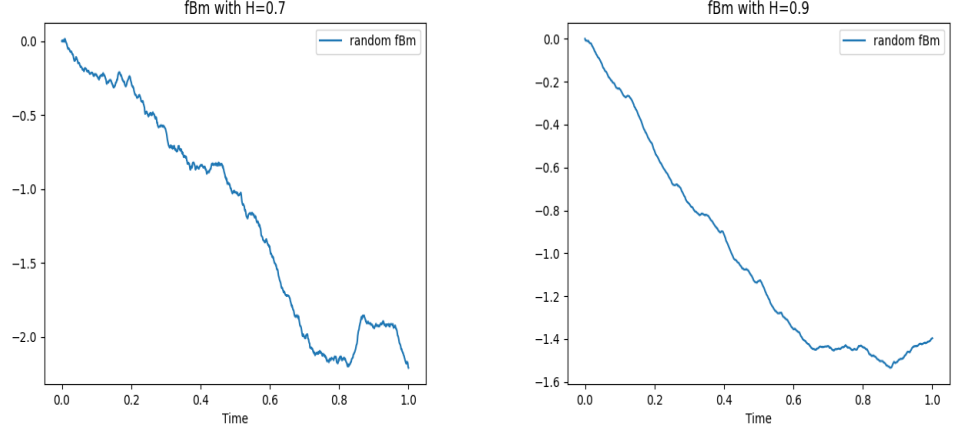
(c) H=0.7   (d) H=0.9
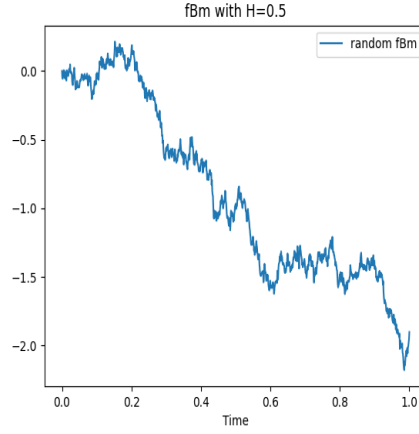
(e) H=0.5 (standard Brownian motion)

Figure 1.0: fractional Brownian motion's paths.

$H-$Hölder continuous.   As we get closer to $H = 1$, the paths become smoother.

We have a very rough behaviour when H is small: when $H < \frac{1}{2}$, we say that the trajecories of the fractional Brownian motion have a "rough behaviour".

There is also the plot of a standard Brownian motion with $H = \frac{1}{2}$, Figure 1.1 (e).

We can also observe the long-range memory effect: when H is small, the range of values assumed by W^H, when the time is between 0 and 1, is wider than the range of values assumed by W^H with higher H. This makes sense,

as with higher values of H, the fBm W^H has better memory of the past. Hence it is expected that it "should not" move too far from previous values in a short time lapse.

Finally we can visualize the reasons for which we denote the case $H < \frac{1}{2}$ as "rough behaviour" of the fractional Brownian motion, while the case $H > \frac{1}{2}$ is known as the "long memory behaviour".

1.2 Riemann-Liouville integrals and derivatives of order α

Fractional derivatives (and integrals) refer to derivatives of order α where α is a real positive number not necessarily integer. There are various definitions of fractional derivatives and integrals. We will discuss the Riemann-Liouville (henceforth R-L) integrals and derivatives, which were, as the name suggests, introduced by Riemann and Liouville.

These generalize the concept of differentiation and integrals. Linearity and semigroup properties are mantained. Moreover, the fractional R-L differential and integral operators are one the inverse of the other. We will see some key properties. For further details see [4].

We start by reminding:

Definition 5 (Gamma Function).
The Gamma function $\Gamma : \mathbb{C} \to \mathbb{R}$ is defined as

$$\Gamma(z) := \int_0^\infty x^{z-1} e^{-x} dx \qquad (1.15)$$

where x is the real part of z.

When we want to integrate n times, there is the known formula (Cauchy formula for repeated integration, see [13]):

$$\int_a^x d\sigma_1 \int_a^{\sigma_1} d\sigma_2 ... \int_a^{\sigma_{n-1}} f(\sigma_n)\, d\sigma_n = \frac{1}{(n-1)!} \int_a^x (x-t)^{n-1} f(t)\, dt. \quad (1.16)$$

And we remind that the Gamma function is strictly related to the factorial: $\Gamma(n) = (n-1)!$. Therefore, the RHS of (1.16) might be generalized to the case $n \in \mathbb{R}_+$. Hence the definition from Riemann and Liouville:

Definition 6 (Riemann-Liouville fractional integral of order $\alpha > 0$).
Given $\alpha > 0$, $t > 0$ and $f \in L^1(0,T)$, the Riemann-Liouville fractional integral of order α is defined as:

$$I_\alpha f(t) := \frac{1}{\Gamma(\alpha)} \int_0^t (t-s)^{\alpha-1} f(s)\, ds, \qquad t \in (0,T) \qquad (1.17)$$

In some books, the operator I_α is also denoted as $D^{-\alpha}$ (being the inverse of the fractional derivative D^α that we are going to define), or I^α. We will stick to I_α as in the main paper [5] on which is based our work. Recall that $f \in L^1(0,T)$ iff $\int_0^T |f(x)|\,dx < \infty$.
Notice that this definition generalizes the case with standard integrals, as for α integer we have exactly the formula (1.16).

Remark 4 (Some useful properties of the R-L fractional integral operator)**.**

• *Notice that the R-L fractional integral operator I_α is a linear operator, as $I_\alpha(f+kg) = I_\alpha(f) + kI_\alpha(g)$ for any $k \in R$ and $f,g \in L^1(0,T)$. The linearity follows immediately from the linearity of the standard integration.*
• *It holds:*

$$I_\alpha I_\beta = I_{\alpha+\beta} \tag{1.18}$$

for any $\alpha, \beta > 0$.

For proof we refer to [4], Part I, section 2.3. This makes of the set $\{I_\alpha | \alpha > 0\}$, a semigroup with respect to the composition operation (induced by the composition of functions' operation) and more importantly it makes of $\alpha \to I_\alpha$ a group homomorphism (where the space $\{\alpha > 0\}$ is given with the usual sum operation).

It is then natural to define the R-L fractional derivative as the inverse operation of the fractional integral (from now on we might omit the "Riemann-Liouville" connotation, as it is clear we only work with these fractional derivatives and integrals).

We follow the approach from [4]: we first define the fractional derivative for $\alpha \in (0,1)$, then we extend it to $\alpha \geq 1$.

Definition 7 (Riemann-Liouville fractional derivative of order $\alpha \in (0,1)$)**.**
Let $\alpha \in (0,1)$ and $t > 0$. Given a function $f : (0,+\infty) \to \mathbb{R}$, we denote by

$$D^\alpha f(t) := \frac{1}{\Gamma(1-\alpha)} \frac{d}{dt} \int_0^t (t-s)^{\alpha-1} f(s)\,ds \tag{1.19}$$

the Riemann-Liouville fractional derivative of f of order α, when it exists.

A sufficient condition for its existence is $f \in AC([0,T])$ (see Lemma 2.2 of [4]).

Now if we want to extend the definition to $\alpha \geq 1$, we have to consider some things: we would like that the fractional derivation is a generalization

of the usual differentiations (α integer), and that the fractional derivatives operators satisfy the semigroup property, namely $D^\alpha D^\beta = D^{\alpha+\beta}$.

Thus it is natural to define the fractional derivative for $\alpha \geq 1$ as:

$$D^\alpha f(t) := \left(\frac{d}{dx}\right)^{\lfloor \alpha \rfloor} D^{\{\alpha\}} f(t) \tag{1.20}$$

where $D^{\{\alpha\}} f(t) = \frac{1}{\Gamma(1-\{\alpha\})} \frac{d}{dt} \int_0^t (t-s)^{\{\alpha\}-1} f(s) \, ds$ by Definition 7, as $0 \leq \{\alpha\} < 1$.

We can write (1.19) and (1.20) in a more concise way. In general, the R-L fractional derivative of order $\alpha > 0$ is

Definition 8 (Riemann-Liouville fractional derivative of order $\alpha \in \mathbb{R}_+$). *We denote by*

$$D^\alpha f(t) = \frac{1}{\Gamma(n-\alpha)} \frac{d^n}{dt^n} \int_0^t (t-s)^{n-1-\alpha} f(s) \, ds, \quad n = \lfloor \alpha \rfloor + 1 \tag{1.21}$$

the Riemann-Liouville fractional derivative of order $\alpha \in \mathbb{R}_+$ of f, when it exists.

A sufficient condition for its existence is $f(x) \in AC^{\lfloor \alpha \rfloor}(0,T)$ (see [4], Chapter I, Theorem 2.2).

This operator is an extension of the usual differential operator. Moreover, it satisfies the property $D^{\alpha+\beta} = D^\alpha D^\beta$ for all $\alpha, \beta > 0$, as a direct consequence of how it has been defined.

Finally, the fractional differential operator D^α is indeed the inverse of the I_α operator. In particular it holds that

Remark 5 (Reciprocal operators)**.**

$$D^\alpha I_\alpha(f) = f \tag{1.22}$$

for any $\alpha > 0$, and for any f for which it makes sense applying the operators D^α and I_α one after the other.

This is a consequence of the Abel's equations (see [4], Chapter I, section 2.3).
However, it is not true that $I_\alpha D^\alpha(f) = f$. In the standard case, differentiating and then integrating a function, returns a function that differs by some constant to the initial function. In the same way, in the fractional case we do not have the identity $I_\alpha D^\alpha(f) = f$.
What we have instead is an expression like

$$I_\alpha D^\alpha f = f + k_\alpha \tag{1.23}$$

where k_α is linear combination of fractional monomial of the type $x^{\alpha-m}$, for $m = 1, 2, \cdots, \lfloor \alpha \rfloor + 1$. For more details, see [4] Chapter 2.6.

1.2.1   Fractional derivatives and integrals of powers

We will see now fractional derivatives and integrals of some elementary functions, in particular for $f(t) = t^r$ where $r \in \mathbb{R}$.

Lemma 2 (Fractional Derivative and Integral of Power functions).
The followings two hold true:

Identity 1 (Fractional Derivative of Power functions).

$$D^\alpha t^r = \frac{\Gamma(r+1)}{\Gamma(r+1-\alpha)} t^{r-\alpha} \tag{1.24}$$

if $r > \alpha - 1$ and $D^\alpha t^{\alpha-1} = 0$.

Identity 2 (Fractional Integral of Power functions).

$$I_\alpha t^r = \frac{\Gamma(r+1)}{\Gamma(r+\alpha+1)} t^{\alpha+r} \tag{1.25}$$

if $r \neq -1$.

Note that the fractional integral and derivative of a power function still remains a power function, modulo some constant. This justifies the use of fractional power series in trying to solve the Riccati equations as we will see later in this work.

Proof. of Lemma 2
Let us prove (1.25) by direct computations: by definition of fractional integral applied to $f(t) = t^r$ $(r \neq -1)$, we have:

$$I_\alpha f(t) = \frac{1}{\Gamma(\alpha)} \int_0^t (t-s)^{\alpha-1} s^r \, ds \tag{1.26}$$

Now let us group the factor t inside the integral:

$$I_\alpha f(t) = \frac{1}{\Gamma(\alpha)} \int_0^t \left(1 - \frac{s}{t}\right)^{\alpha-1} \left(\frac{s}{t}\right)^r t^{\alpha+r-1} \, ds.$$

Now define $z := \frac{s}{t}$ and get

$$I_\alpha f(t) = \frac{1}{\Gamma(\alpha)} \int_0^1 (1-z)^{\alpha-1} z^r t^{\alpha+r} \, dz = \frac{1}{\Gamma(\alpha)} t^{\alpha+r} \int_0^1 (1-z)^{\alpha-1} z^r \, dz.$$

We recognize the Beta function:

$$I_\alpha f(t) = \frac{1}{\Gamma(\alpha)} B(r+1, \alpha) t^{\alpha+r}$$

and by using the property $B(x,y) = \frac{\Gamma(x)\Gamma(y)}{\Gamma(x+y)}$, we get

$$I_\alpha f(t) = \frac{1}{\Gamma(\alpha)} \frac{\Gamma(\alpha)\Gamma(r+1)}{\Gamma(\alpha+r+1)} t^{\alpha+r} = \frac{\Gamma(r+1)}{\Gamma(\alpha+r+1)} t^{\alpha+r}$$

which is equation (1.25).

The differential version (1.24) is then a direct consequence of (1.25) together with the inversion formula $D^\alpha I_\alpha f = f$. ∎

1.2.2 Rewriting in integral form the Riccati differential equation

Following the work of [5], instead of working with the Riccati in its differential form, we will be working with the equivalent integral version. In particular, under appropriate integrability conditions on the functions ψ^2 and ψ, we have the equivalent integral Riccati equations.

For $\alpha \in (0,1]$, the Riccati differential equation $\mathcal{E}^u_{\lambda,\mu,\nu}$ (defined in eq. (11)), becomes:

$$\psi(t) = \frac{u}{\Gamma(\alpha)} t^{\alpha-1} + I_\alpha(\lambda\psi^2 + \mu\psi + \nu), \qquad (1.27)$$

while for $\alpha \in (1,2]$, the Riccati differential equation $\mathcal{E}^{u,v}_{\lambda,\mu,\nu}$ becomes the equivalent integral Riccati equation:

$$\psi(t) = \frac{u}{\Gamma(\alpha)} t^{\alpha-1} + \frac{v}{\Gamma(\alpha-1)} t^{\alpha-2} + I_\alpha(\lambda\psi^2 + \mu\psi + \nu). \qquad (1.28)$$

Notice that when we integrate we introduce the initial conditions inside the equations through the inversion formula (1.23), by considering that, $I_{1-\alpha}\left(\frac{u}{\Gamma(\alpha)} t^{\alpha-1}\right) = u$ and $I_{2-\alpha}\left(\frac{v}{\Gamma(\alpha)} t^{\alpha-2}\right) = v$ due to the integral formula for power series (1.25).

Chapter 2

Riccati's solution as Power Series

In this chapter we will express the solution to the Riccati fractional differential equation $\mathcal{E}^0_{\lambda,\mu,\nu}$ (eq. (11)), namely with $\alpha \in (0,1]$ and null initial condition $I_{1-\alpha}\psi(0) = 0$, as a fractional power series. The homogeneous case (i.e., null initial condition) is simpler than the non-homogeneous case, which is solved through a double index series in [5]. Moreover, the homogeneous case has wider applications in Finance than the non-homogeneous case.
As anticipated at the beginning, the Riccati differential equation $\mathcal{E}^{u,v}_{\lambda,\mu,\nu}$ (defined in eq. (11)) has a unique solution (see [3]).

If we denote by D_ψ the maximal domain of existence for the solution ψ to $\mathcal{E}^0_{\lambda,\mu,\nu}$, and R_ψ the radius of convergence of the fractional power series solution, then $\mathcal{D}(0, R_\psi) \subseteq D_\psi$ (where $\mathcal{D}(0, R_\psi)$ denotes the open disk centered in 0 of radius R_ψ). In particular the solution could exist outside the convergence radius of the fractional series. In this case we will use the Euler scheme (illustrated in the next chapter), which is a method that approximates the solution $\psi(t)$ to the Riccati differential equation with a sequence $\{\bar{\psi}^n\}_{n\geq 1}$ of discrete functions.

We will focus solely on the case $t \geq 0$ from now on, though general results related to convergence also hold for $t \in \mathbb{C}$.

Assume that

$$\psi(t) = \psi_{\lambda,\mu,\nu}(t) := \sum_{k=0}^{\infty} a_k t^{k\alpha} \tag{2.1}$$

is a solution to $\mathcal{E}^0_{\lambda,\mu,\nu}$:

$$D^\alpha \psi(t) = \lambda\psi^2 + \mu\psi + \nu, \quad I_{1-\alpha}\psi(0) = 0, \ \alpha \in (0,1]. \tag{2.2}$$

We will impose (2.2) on (2.1) so that we can find explicitly the coefficients a_k. This does not guarantee that $\psi(t)$ is a solution to (2.2). It does satisfy

the necessary conditions for being a solution to (2.2), but we are not sure that the series is a well defined function, as it might diverge for some $t \in \mathbb{R}_+$ (we are interested only in the positive real axis). We also need to check that its convergence radius is positive, so that it is at least well defined in a non empty disk, where it absolutely converges (for $|t| < R_\psi$, while for $t = R_\psi$ we do not know the behaviour a priori).

We first find explicitly the coefficients a_k, subsequently we will discuss about the existence of the solution and the convergence radius.

We first recall the Cauchy-Hadamard's formula for computing the radius of convergence R_ψ.

Lemma 3 (Cauchy-Hadamard's formula.)**.** *The radius of convergence R_ψ for the fractional power series $\psi(t) = \sum_{k \geq 0} a_k t^{k\alpha}$ is given by the formula:*

$$R\psi = \liminf_{k \geq 0} |a_k|^{-\frac{1}{\alpha k}}. \tag{2.3}$$

As a final observation, notice that if $\nu = 0$, then $\psi(t) \equiv 0$ satisfies $\mathcal{E}^0_{\lambda,\mu,\nu}$. By uniqueness we deduce that this is the only solution to the Riccati $\mathcal{E}^0_{\lambda,\mu,0}$. So, from now on we will suppose $\nu \neq 0$.

2.1   Finding the coefficients

Let us assume that the convergence radius $R_\psi > 0$ (we will discuss it later), in which case, for $t \geq 0$ such that $R_\psi > t$, the series converges absolutely. Moreover, if $R_\psi > 0$, it also makes sense to talk about the series ψ^2, or the Cauchy product of the series $\psi(t) = \sum_{k=0}^{\infty} a_k t^{k\alpha}$ with itself. Indeed, for any $t \geq 0$ s.t. $R_\psi > t$, the Cauchy product is well defined, as both the factors (in this case the same series) are absolutely convergent within the convergence radius (see Theorem 3.50, p. 74 in [10]).

Hence

$$\psi^2(t) = \sum_{k \geq 0} a_k^{*2} t^{k\alpha}, \tag{2.4}$$

where the coefficients a_k^{*2} of the Cauchy product are given by the convolution of the coefficients a_k:

$$a_k^{*2} = \sum_{l=0}^{k} a_l a_{k-l}, \quad k \geq 0. \tag{2.5}$$

Now, recalling the fractional derivative of a power function in equation (1.24), it follows that

$$D^\alpha \psi(t) = \sum_{k \geq 0} a_k \frac{\Gamma(\alpha k + 1)}{\Gamma(\alpha k + 1 - \alpha)} t^{\alpha(k-1)} \tag{2.6}$$

where $\alpha \in (0,1]$. Note that this is in analogy with the formal standard derivative of a series (for $|t| < R_\psi$, the formal derivative of a series is convergent, as it has the same radius of convergence R_ψ), where in our case the fractional derivative of the series becomes a series of fractional derivatives.

Now, given the Riccati equation structure $\mathcal{E}^0_{\lambda,\mu,\nu}$ and (2.4), it follows that

$$D^\alpha \psi(t) = \lambda \psi^2(t) + \mu \psi(t) + \nu = \sum_{k \geq 0} (\lambda a_k^{*2} + \mu a_k) t^{\alpha k} + \nu, \qquad (2.7)$$

so that we can compare (2.7) and (2.6) and equate the coefficients that have the same power $t^{\alpha k}$. This is justified by the theory of complex series within their convergence radius, namely, if two series are equal within a portion of their convergence domain, then their coefficients are equal in that portion of domain. Comparing the two series gives us a recurrent relation on the coefficients a_k:

$$(A_{\lambda,\mu,\nu}) \equiv \begin{cases} a_{k+1} = (\lambda a_k^{*2} + \mu a_k) \frac{\Gamma(\alpha k + 1)}{\Gamma(\alpha k + \alpha + 1)}, & k \geq 1, \\ a_1 = \frac{\nu}{\Gamma(\alpha+1)}, \\ a_0 = 0, \end{cases} \qquad (2.8)$$

where we remind that a_k^{*2} solely depends on the coeffients a_l for $l \leq k$. The relation $(A_{\lambda,\mu,\nu})$ determines uniquely the coefficients a_k of the fractional power series. Notice also that since $a_0 = 0$, then $\psi(0) = 0$, which is our initial condition.

2.2 Radius of Convergence

So far we assumed that the radius of convergence R_ψ is greater than zero in order to find the relations on the coefficients a_k given in $(A_{\lambda,\mu,\nu})$. The fact that $R_\psi > 0$ is justified by the following theorem, whose proof will be omitted (for reference see [5]):

Theorem 2. Let $\alpha \in [0,2]$, $\lambda, \mu, \nu \in \mathbb{C}$ and $\lambda \neq 0$. Let $\psi_{\lambda,\mu,\nu} = \sum_{k \geq 0} a_k t^{k\alpha}$, where the coefficients a_k satisfy (2.8). Then
i) [lower bound radius] we have

$$0 < \tau_* := \frac{2^{\frac{1}{\alpha} - (\frac{1}{\alpha} - 2)^+} \alpha}{\left(|\mu| + \sqrt{\mu^2 + c_\alpha \frac{|\lambda||\nu|}{\Gamma(\alpha)}} \right)^{\frac{1}{\alpha}}} < R_{\psi_{\lambda,\mu,\nu}} \qquad (2.9)$$

where $c_\alpha = 2^{2 - (1-2\alpha)^+ - 2(\alpha-1)^+} \alpha^{\alpha-1} B(\alpha \wedge 1, \alpha \wedge 1) > 0$. Notice that τ_* depends only on the coefficients of the Riccati equation and on the order of differentiation α.

ii) [upper bound radius] if $\mu \geq 0$, $\lambda, \nu > 0$ (respectively $\mu \leq 0$, $\lambda, \nu < 0$), then

$$R_{\psi_{\lambda,\mu,\nu}} \leq R_{\psi_{|\lambda|,0,|\nu|}} \leq C_\alpha \left(\frac{\Gamma(\alpha + 1)}{\lambda \nu} \right)^{\frac{1}{2\alpha}}$$

where

$$C_\alpha = \begin{cases} (3.5^{\alpha-1}) * \frac{1}{2\alpha}\sqrt{\alpha} & if\ \alpha \in (0,1] \\ \frac{\sqrt{2\alpha}}{\tilde{B}(\alpha)} & if\ \alpha \in (1,2] \end{cases}$$

where $\tilde{B}(\alpha) = B(\alpha, \alpha) - 2^{1-2\alpha} > 0$. Moreover, $\psi_{\lambda,\mu,\nu}$ is increasing (respectively decreasing) for t such that $R_{\psi_{\lambda,\mu,\nu}} > t \geq 0$. And we also have

$$\lim_{t \to +R_{\psi_{\lambda,\mu,\nu}}} \psi_{\lambda,\mu,\nu}(t) = sgn(\lambda) \cdot \infty.$$

This theorem grants us that the radius of convergence is positive if $\lambda \neq 0$. We wonder what happens if $\lambda = 0$.

2.2.1   Particular Case $\lambda = 0$

If $\lambda = 0$, then we will show that the radius of convergence $R_\psi = +\infty$ (i.e., the series converges absolutely everywhere).

Let $\lambda = 0$, then by $(A_{\lambda,\mu,\nu})$ we easily get by induction

$$a_{k+1} = \nu \frac{\mu^k}{\Gamma(\alpha(k+1)+1)}, \tag{2.10}$$

for any $k \geq 1$. In particular, if $\mu = 0$ then $a_{k+1} \equiv 0$ for any $k \geq 1$. Thus the series converges absolutely everywhere $(R_\psi = +\infty)$. Assume now $\mu \neq 0$.

Consider the limit

$$\lim_{k \to +\infty} |a_k|^{-\frac{1}{\alpha k}} =$$

$$\lim_{k \to +\infty} \left(\frac{|\nu||\mu|^{k-1}}{\Gamma(k\alpha + 1)} \right)^{-\frac{1}{\alpha k}} = \tag{2.11}$$

$$\lim_{k \to +\infty} \frac{1}{|\mu|^{\frac{k-1}{\alpha k}}} \cdot \frac{1}{|\nu|^{\frac{1}{\alpha k}}} \cdot (\Gamma(\alpha k + 1))^{\frac{1}{\alpha k}}.$$

We want to prove that this limit (2.11) is $+\infty$, which, by Hadamard's formula (Lemma 3) means $R_\psi = +\infty$.

The first product $\frac{1}{|\mu|^{\frac{k-1}{\alpha k}}} \cdot \frac{1}{|\nu|^{\frac{1}{\alpha k}}}$ converges to $\frac{1}{|\mu|^{\frac{1}{\alpha}}} > 0$ as $k \to +\infty$ (remind that $\alpha \in (0, 2)$ and $\mu, \nu \neq 0$):

$$\lim_{k \to +\infty} \frac{1}{|\mu|^{\frac{k-1}{\alpha k}}} \cdot \frac{1}{|\nu|^{\frac{1}{\alpha k}}} = \frac{1}{|\mu|^{\frac{1}{\alpha}}} > 0.$$

Thus, the limit (2.11) is $+\infty$, if and only if, $(\Gamma(\alpha k + 1))^{\frac{1}{\alpha k}} \to +\infty$ as $k \to +\infty$. In order to prove this, we will show the following:

Corollary 1.
Let Γ be the Gamma function. Then

$$\lim_{x \to +\infty} \Gamma(x)^{\frac{1}{x-1}} = +\infty. \tag{2.12}$$

It is clear that if this holds, then the limit (2.11) converges to $+\infty$ (set $x := \alpha k + 1$, then $(\Gamma(\alpha k + 1))^{\frac{1}{\alpha k}} = \Gamma(x)^{\frac{1}{x-1}}$).

In order to prove Corollary 1, we will use Nemes' formula (Corollary 4.1 from [14]):

Corollary 2 (Nemes' formula)**.**
Let Γ be the Gamma function. Then, for $x \to +\infty$, it holds the following asymptoticity:

$$\Gamma(x) \sim \left(\frac{x}{e}\right)^x \sqrt{\frac{2\pi}{x}} \left(1 + \frac{1}{12x^2 - \frac{1}{10}}\right)^x. \tag{2.13}$$

Now let us prove Corollary 1.

Proof. of Corollary 1.
Using Nemes' formula (Corollary 2) we get, for $x \to +\infty$:

$$\Gamma(x)^{\frac{1}{x-1}} \sim \frac{x^{\frac{x-\frac{1}{2}}{x-1}}}{e^{\frac{x}{x-1}}} \cdot \sqrt{2\pi}^{\frac{1}{x-1}} \cdot \left(1 + \frac{1}{12x^2 - \frac{1}{10}}\right)^{\frac{x}{x-1}}. \tag{2.14}$$

It is clear that the product $\frac{x^{\frac{x-\frac{1}{2}}{x-1}}}{e^{\frac{x}{x-1}}} \cdot \sqrt{2\pi}^{\frac{1}{x-1}}$ converges to $+\infty$ as $x \to +\infty$:

$$\lim_{x \to +\infty} \frac{x^{\frac{x-\frac{1}{2}}{x-1}}}{e^{\frac{x}{x-1}}} \cdot \sqrt{2\pi}^{\frac{1}{x-1}} = +\infty, \tag{2.15}$$

and $\left(1 + \frac{1}{12x^2 - \frac{1}{10}}\right)^{\frac{x}{x-1}}$ converges to 1 as $x \to +\infty$:

$$\lim_{x \to +\infty} \left(1 + \frac{1}{12x^2 - \frac{1}{10}}\right)^{\frac{x}{x-1}} = 1. \tag{2.16}$$

Finally, using (2.14), (2.15) and (2.16), we get:

$$\lim_{x \to +\infty} \Gamma(x)^{\frac{1}{x-1}} = \lim_{x \to +\infty} \frac{x^{\frac{x-\frac{1}{2}}{x-1}}}{e^{\frac{x}{x-1}}} \cdot \sqrt{2\pi}^{\frac{1}{x-1}} \cdot \left(1 + \frac{1}{12x^2 - \frac{1}{10}}\right)^{\frac{x}{x-1}} = +\infty,$$

which is (2.12).   ∎

This concludes the fact that $\lambda = 0$ implies $R_\psi = +\infty$, namely, the series converges absolutely everywhere.

2.2.2   About Accuracy and Truncation of the series

There is a final note about the accuracy in truncating the fractional power series, as making numerical tests will not allow us to have infinite sums. In this regard, there are some estimates that measure the accuracy of the fractional power series truncated up to the n_0-th coefficient (we will consider $\sum_{k=0}^{n_0} a_k t^{k\alpha}$ in place of $\sum_{k=0}^{+\infty} a_k t^{k\alpha}$). The accuracy, or relative distance from the real value, is affected by n_0. Later we will see the formula (3.5), which gives the least n_0-th coefficient up to which we have to truncate the series in order to attain a desired accuracy $\epsilon_0 \geq 0$. For further details see [5].

Recapitulating, by imposing $\mathcal{E}^0_{\lambda,\mu,\nu}$ on $\psi(t) = \sum_{k \geq 1} a_k t^{k\alpha}$, we determined the coefficients a_k (a recurrent relation $(A_{\lambda,\mu,\nu})$ on a_k). Moreover, since the convergence radius is positive by Theorem 2, the series $\psi(t) = \sum_{k \geq 1} a_k t^{k\alpha}$ is well defined within its convergence radius. Therefore, for $|t| < R_\psi$, the series whose coefficients are determined by $(A_{\lambda,\mu,\nu})$, satisfies to $\mathcal{E}^0_{\lambda,\mu,\nu}$ (by construction), being then a solution. Nevertheless, knowing that the solution exists and it is unique (see [3]), this has to be exactly the solution.

There is a limitation in this: the fractional power series centered at zero is only defined within R_ψ, while the solution might exist over R_ψ. For this we will apply an hybrid approach in Chapter 3.

Chapter 3

Euler Discretization Scheme

In the previous chapter we expressed the solution to $\mathcal{E}^0_{\lambda,\mu,\nu}$ (eq. (11)) as a fractional power series. However, the solution could be defined in a larger domain than the power series' domain of absolute convergence (i.e., a disk centered in 0). For this reason we apply an Euler scheme that approximates the solution ψ. This scheme aims to define the solution in a broader domain through a sequence of piecewise step functions $\left\{\bar{\psi}^n\right\}_{n\in\mathbb{N}}$ that converges to the solution ψ. The whole approach will be hybrid in the sense that within a threshold (to be specified as below in Section 3.2) we still use the fractional power series, while outside of that threshold we will use the Euler scheme.

We remind that we focus our analysis for $T > 0$ such that $T \in D_\psi$ (i.e., T is in D_ψ, the maximal domain of existence of the solution). For such a $T > 0$ fixed, we will approximate $\psi(T)$ with some functions $\bar{\psi}^n(T)$ that converge to $\psi(T)$ as $n \to +\infty$.

We recall that
$$\psi(t) = \sum_{r \geq 1} a_r t^{\alpha r}$$
within the disk $\mathcal{D}(0, \widehat{R_\psi})$. From this we get, reminding the identity for fractional integrals of power functions (1.25) and letting $f_r(t) := t^{r\alpha}$:

$$
\begin{aligned}
I_{1-\alpha}(\psi)(t) &= \sum_{r \geq 1} a_r I_{1-\alpha}(f_r)(t) \\
&= \sum_{r \geq 1} a_r \frac{\Gamma(\alpha r + 1)}{\Gamma(\alpha r - \alpha + 1)} \cdot \frac{t^{\alpha r + 1 - \alpha}}{(\alpha r + 1 - \alpha)} \\
&= t^{1-\alpha} \left(\nu t^\alpha + \sum_{r=2}^{\infty} a_r \left(1 - \frac{1}{r}\right)^{-1} \frac{\Gamma(\alpha r) t^{r\alpha}}{\Gamma(\alpha r - \alpha) \cdot (\alpha r + 1 - \alpha)} \right)
\end{aligned}
$$
(3.1)

where in the last equality we substituted the values of a_0 and a_1 from $(A_{\lambda,\mu,\nu})$

in equation (2.8).

In practical cases, we will be using Hadamard's formula to get an estimate of the radius of convergence R_ψ. Let us see how we estimate it.

3.1 Estimates of the radius R_ψ and accuracy

We do not have only one way of estimating the radius of convergence R_ψ: we will discuss two estimates. Let us see into more details.

3.1.1 Two estimates for the radius of convergence R_ψ

By Hadamard's formula, we know that the radius of convergence R_ψ is given by

$$R_\psi := \liminf_{r \geq 0} |a_r|^{-\frac{1}{\alpha r}} = \lim_{r \to +\infty} \left(\inf_{m \geq r} |a_m|^{-\frac{1}{\alpha m}} \right).$$

Since we cannot compute all the coefficients a_m ($m \in \mathbb{N}$), we will have to estimate R_ψ. In particular, if we compute the first r_{max} coefficients (where $r_{max} \in \mathbb{N}$ is arbitrary, even though later we pick it as in (3.5) with $r_{max} = r_0$, in order to attain a desired accuracy), we will have an estimate:

Estimate Radius 1.

$$R_\psi^{r_{max}} := |a_{r_{max}}|^{-\frac{1}{\alpha r_{max}}} \tag{3.2}$$

Note that this might overestimate R_ψ, as well as underestimate it, as the sequence of coefficients $\{a_m\}_{m \in \mathbb{N}}$ might not be monotone.
Now, if we consider the fractional series $I_{1-\alpha}(\psi)(t)$ (see (3.1)), then this has the same radius of converence as of the fractional series $\psi(t) = \sum_{k \geq 0} a_k t^{k\alpha}$, by the general theory of complex power series (which also holds in the fractional case, as the fractional integral $I_{1-\alpha}$ is defined through standard integrations).
If we denote by a'_r the coefficients of the series $I_{1-\alpha}(\psi)(t)$ (see (3.1)), then

$$a'_r = a_r \frac{\Gamma(\alpha r + 1)}{\Gamma(\alpha r - \alpha + 1)} \frac{1}{\alpha r + 1 - \alpha}. \tag{3.3}$$

Therefore we can have (see below eq. (3.4)) an alternative estimate $\widehat{R}_\psi$ for the radius R_ψ.

Estimate Radius 2. A second possible estimate is:

$$\widehat{R}_\psi := |a'_{r_{max}}|^{-\frac{1}{\alpha r_{max}}}. \tag{3.4}$$

We prefer using this estimate $\widehat{R}_\psi$, as they do in paper [5].

3.1.2   Accuracy In truncating

So far, truncating and having an approximate radius of convergence is not enough: we also need a measure of accuracy for the truncated series, where by accuracy we mean the maximum relative distance to the real value inside the disk $\mathcal{D}(0, \widehat{R}_\psi)$. Namely, if we denote by $\tilde{\psi}(t) := \sum_{k=k_0}^{n} a_k t^{k\alpha}$ the truncated series and ψ the solution to the Riccati equation $\mathcal{E}^0_{\lambda,\mu,\nu}$ (eq. (11)), then $d(\tilde{\psi}, \psi)(t) := \left| \frac{\tilde{\psi}(t) - \psi(t)}{\tilde{\psi}(t)} \right|$ is our precision in t, where $|t| < \widehat{R}_\psi$. The accuracy is the sup of the precisions in t for $t \in \mathcal{D}(0, \widehat{R}_\psi)$: $\sup_{|t| < \widehat{R}_\psi} d(\tilde{\psi}, \psi)(t)$. Let ϵ_0 be our accuracy (typically $\epsilon_0 = 0.01$). If we want the value of the series in t, for t close to the estimate $\widehat{R}_\psi$, we will need to compute more terms of the series in order to attain the desired precision, which is not uniform in t. For this reason we move a bit away from the threshold $\widehat{R}_\psi$, by taking $\theta \in (0,1)$ and considering the truncated series for $t \in [0, \theta\widehat{R}_\psi]$. Moreover the accuracy will be intended to the restricted disk $\mathcal{D}(0, \theta\widehat{R}_\psi)$. In the numerical tests in section 4.1 we use $\theta = 0.9$.

The desired accuracy is attained by truncating up to the first r_0 coefficients, where r_0 is given by

$$r_0 = r_0(\epsilon_0, \theta) = \left\lceil \frac{log(\epsilon_0(1-\theta))}{\alpha \log(\theta)} - 1 \right\rceil \tag{3.5}$$

This formula is given in [5], which is determined empirically.

Now we can proceed to our hybrid expansion with the Euler discretization scheme.

3.2   Hybrid Expansion

As discussed in the previous subsection 3.1.2, we keep us far from the estimate $\widehat{R}_\psi$ by setting the threshold to $\theta\widehat{R}_\psi$ in order to have enough accuracy in the series expansion.

If we want to compute $\psi(T)$, we have two cases based on the value of T (which we remind being positive and belonging to D_ψ, the maximal domain of existence of the solution ψ.).

3.2.1   Case 1: $T < \theta\widehat{R}_\psi$.

If $T < \theta\widehat{R}_\psi$, we simply evaluate the truncated fractional power series (whose coefficients satisfy $(A_{\lambda,\mu,\nu})$) in T and set the result as the value assumed by $\psi(T)$.

3.2.2 Case 2: $T > \theta \widehat{R}_\psi$.

If $T > \theta \widehat{R}_\psi$, we use the Euler discretization scheme, which we are going to introduce below.

Let $n \geq 1$ be a fixed integer. We denote by $\bar{\psi}^n$ the n-th Euler discretization of ψ. This is an estimate of ψ and is a piecewise step function assuming at most $n \in \mathbb{N}$ different values (namely, a finite linear combination of indicator functions of intervals). As n increases, the estimate $\bar{\psi}^n$ becomes more and more accurate.

We divide the disk $\mathcal{D}(0, T)$ into circular areas with increasing radius of fixed step $h = \frac{T}{n}$, where $n \geq 1$ integer. We set

$$t_k = t_k^n := \frac{kT}{n}, \quad k = 0, ..., n, \quad and \ \ k_0 := \left\lfloor \frac{n\theta \widehat{R}_\psi}{T} \right\rfloor. \qquad (3.6)$$

Note that k_0 is such that $t_{k_0} \leq \theta \widehat{R}_\psi < t_{k_0+1}$, i.e. it is the largest integer s.t. t_{k_0} is smaller than the threshold $\theta \widehat{R}_\psi$.

The function $\bar{\psi}^n$ is a discrete function and first we define it in the set $\{t_k | k = 0, ..., n\}$, then we extend it to the whole interval $(t_0, t_n) = (0, T)$ as a piecewise step function (if $t \in [t_l, t_{l+1})$ we set $\bar{\psi}^n(t) = \bar{\psi}^n(t_l)$).

So how do we define the values of $\bar{\psi}^n(t_k)$ for $k = 0, \cdots, n$?

We use the power series expansion up to $\theta \widehat{R}_\psi$. Subsequently, we consider the integral form of the Riccati equation $(\mathcal{E}^0_{\lambda,\mu,\nu})$, namely

$$\psi = I_\alpha \left(\lambda \psi^2 + \mu\psi + \nu \right).$$

In particular, for the values k such that $0 \leq k \leq k_0$, we set $\bar{\psi}^n(t_k)$ equal to the value computed with the fractional power expansion truncated at r_0 and evaluated at t_k.

In order to compute the other values $\bar{\psi}^n(t_k)$, for $k \in \{k_0 + 1, k_0 + 2, \cdots, n\}$, we use the following Euler Scheme:

3.2.3 Euler Scheme

Given the integral form of the Riccati $\mathcal{E}^0_{\lambda,\mu,\nu}$:

$$\psi(t) = \frac{\nu t^\alpha}{\Gamma(\alpha + 1)} + \frac{1}{\Gamma(\alpha)} \int_0^t \psi(s)(\mu + \lambda\psi(s))(t - s)^{\alpha-1} \, ds, \qquad (3.7)$$

being n fixed, we can compute the values $\bar{\psi}^n(t_k)$ for $k = k_0 + 1, \cdots, n$ by recurrence on $k \geq k_0 + 1$ through the formula:

$$
\begin{aligned}
\bar{\psi}^n(t_k) &= \frac{\nu t_k^\alpha}{\Gamma(\alpha+1)} + \frac{1}{\Gamma(\alpha)} \sum_{l=1}^{k-1} \bar{\psi}^n(t_l) \left(\lambda \bar{\psi}^n(t_l) + \mu\right) \int_{t_l}^{t_{l+1}} (t_k - s)^{\alpha-1} \, ds \\
&= \frac{1}{\Gamma(\alpha+1)} \left(\frac{t}{n}\right)^\alpha \left(\nu k^\alpha + \sum_{l=1}^{k-1} c_{k-l-1}^{(\alpha)} \bar{\psi}^n(t_l) \left(\lambda \bar{\psi}^n(t_l) + \mu\right)\right)
\end{aligned}
$$

(3.8)

with

$$
c_0^{(\alpha)} = 1 \quad and \quad c_l^{(\alpha)} = (l+1)^\alpha - l^\alpha, \quad for \ \ l = 1, \cdots, k-2.
$$

This formula (3.8) follows from the integral Riccati formula (3.7). We substituted t with t_k and ψ with $\bar{\psi}^n$. Then we know how $\bar{\psi}^n$ is defined up to t_{k-1} and we can compute recursively the value in t_k, as $\bar{\psi}^n$ is a piecewise step function.

Moreover, notice that the last equality in (3.8) holds since

$$
\int_{t_l}^{t_{l+1}} (t_k - s)^{\alpha-1} = \frac{(t_k - t_l)^\alpha - (t_k - t_{l+1})^\alpha}{\alpha} = \left(\frac{t}{n}\right)^\alpha \frac{1}{\alpha} \left((k-l)^\alpha - (k-l-1)^\alpha\right)
$$

where we used the definition of t_k and the property of the Gamma function $\frac{\Gamma(\alpha)}{\Gamma(\alpha+1)} = \frac{1}{\alpha}$ for any $\alpha > 0$.

3.2.4 How good does $\bar{\psi}^n$ approximate ψ?

There is not a theoretical estimate yet, but sperimental tests strongly suggest that

$$
\bar{\psi}^n(T) - \psi(T) = \frac{c_1}{n} + o(n^{-1})
$$

(3.9)

for a constant c_1. If this estimate holds true, we can also estimate the value of c_1.

Remark 6. *Assuming the validity of (3.9), we get that the sequence* $\{\bar{c_1}^n\}_{n \in N}$ *defined as*

$$
\bar{c}_1^n := 2n \left(\bar{\psi}^n(T) - \bar{\psi}^{2n}(T)\right)
$$

(3.10)

convergese to c_1 as $n \to +\infty$.

Indeed

$$
\begin{aligned}
\bar{c}_1^n &= 2n \left(\bar{\psi}^n(T) - \bar{\psi}^{2n}(T)\right) \\
&= 2n \left(\left(\bar{\psi}^n(T) - \psi(T)\right) - \left(\bar{\psi}^{2n}(T) - \psi(T)\right)\right) \\
&= 2n \left(\frac{c_1}{n} - \frac{c_1}{2n} + o(n^{-1})\right) \\
&= c_1 + 2n \cdot o(n^{-1}) \to c_1
\end{aligned}
$$

as $n \to \infty$ since $n \cdot o(n^{-1}) \to 0$ as $n \to \infty$.

Summarizing, we approximated $\psi(T)$ with $\bar{\psi}^n(T)$ through an hybrid method consisting of the fractional series expansion and the Euler scheme. Having the estimate $\bar{\psi}^n(T)$ of $\psi(T)$ is yet a considerable result, especially for large values of n. Nevertheless we can have a faster convergence through an extrapolation if the measure (3.9) holds true. This happens with the extrapolated hybrid method that we will see in the next section:

3.3   Extrapolated Hybrid Method

If we assume true the error estimate (3.9), then, from the hybrid Euler expansion we can get an approximator for $\psi(T)$, namely the Richardson-Romberg Approximator:

$$\bar{\psi}^n_{RR,2}(T) := 2\bar{\psi}^n(T) - \bar{\psi}^{\frac{n}{2}}(T) \tag{3.11}$$

defined for n even.

The Richardson-Romberg approximator $\bar{\psi}^n_{RR,2}(T)$, extracted from the Euler approximator $\bar{\psi}^n(T)$, converges faster than the latter. Indeed it holds that

$$\begin{aligned}
\bar{\psi}^n_{RR,2}(T) - \psi(T) &= 2\left(\bar{\psi}^n(T) - \psi(T)\right) - \left(\bar{\psi}^{n/2}(T) - \psi(T)\right) \\
&= 2\left(\frac{c_1}{n} + o(n^{-1})\right) - \left(\frac{c_1}{n/2} + o(n^{-1})\right) \\
&= o(n^{-1}),
\end{aligned}$$

which goes to zero faster than (3.9), as $n \to +\infty$, meaning that the Richardson-Romber approximator $\bar{\psi}^n_{RR,2}(T)$ converges to the solution ψ more quickly than the Euler approximator $\bar{\psi}^n$.

3.3.1   Multistep extrapolated hybrid method

Let us assume that in place of (3.9) there is a more accurate estimate of the error, namely

$$\bar{\psi}^n(T) - \psi(T) = \frac{c_1}{n} + \frac{c_2}{n^2} + o(n^{-2}) \tag{3.12}$$

for some constants c_1, c_2.
Then we can apply a multistep Richardson-Romberg extrapolation (for more details see [15]):

$$\bar{\psi}^n_{RR,3}(T) := \frac{1}{3}\bar{\psi}^{n/4}(T) - 2\bar{\psi}^{n/2}(T) + \frac{8}{3}\bar{\psi}^n(T) \tag{3.13}$$

defined for n multiple of four and where the weights $\frac{1}{3}$, -2 and $\frac{8}{3}$ are not chosen randomly (see [15]). With these weights, it follows

$$
\begin{aligned}
\bar{\psi}^n_{RR,3}(T) - \psi(T) &= \frac{1}{3}\left(\bar{\psi}^{n/4}(T) - \bar{\psi}(T)\right) - 2\left(\bar{\psi}^{n/2}(T) - \bar{\psi}(T)\right) + \frac{8}{3}\left(\bar{\psi}^n(T) - \bar{\psi}(T)\right) \\
&= \frac{1}{3}\left(\frac{4c_1}{n} + \frac{16c_2}{n^2}\right) - 2\left(\frac{2c_1}{n} + \frac{4c_2}{n^2}\right) + \frac{8}{3}\left(\frac{c_1}{n} + \frac{c_2}{n^2}\right) + o(n^{-2}) \\
&= o(n^{-2}),
\end{aligned}
$$

$$(3.14)$$

which would make of it an even better approximator than $\bar{\psi}^n_{RR,2}(T)$, as it converges to the solution ψ faster than $\bar{\psi}^n_{RR,2}(T)$.

Summarizing, in order to find the solution ψ to the Riccati fractional differential equation $\mathcal{E}^0_{\lambda,\mu,\nu}$ (eq. (11)), we use the fractional power series (truncated), which is defined inside the bound $\theta\widehat{R}_\psi$. The solution can even be defined outside the disk $\mathcal{D}(0, \theta\widehat{R}_\psi)$ through the Euler discretization scheme: a sequence $\{\bar{\psi}^n\}_{n\in\mathbb{N}}$ is defined (as in Section 3.2) such that it converges to ψ as $n \to +\infty$. Finally, assuming true (3.9) or (3.11), from the sequence $\{\bar{\psi}^n\}_{n\in\mathbb{N}}$ we could extract another sequence $\left\{\bar{\psi}^n_{RR,2}\right\}_{n\in\mathbb{N}}$ (or $\left\{\bar{\psi}^n_{RR,3}\right\}_{n\in\mathbb{N}}$) through the Richardson-Romberg technique such that converges to ψ (as $n \to +\infty$) faster than the sequence $\{\bar{\psi}^n\}_{n\in\mathbb{N}}$.

In the next chapter we will see a practical sperimentation to get a hang of this procedure and see how things look like.

Chapter 4

Numerical Test: Hybrid Euler scheme.

In this chapter we will run some numerical tests to get a feeling of how the Euler scheme works. For code refer to Appendix.

We will run our first experimentation with the following parameters (which are also found in real applications. See [5]):

$$\alpha = 0.64, \ \ \lambda = 0.045, \ \ \mu = -64.938, \ \ \nu = 44850. \tag{4.1}$$

Note that to $\alpha = 0.64$ corresponds $H = \alpha - \frac{1}{2} = 0.14$, which contains the rough behaviour of the fractional Brownian motion.
We will consider $\psi : \mathbb{R}_+ \to \mathbb{R}$.

4.1   General Procedure

Let n be fixed. The general procedure to compute $\bar{\psi}^n(T)$ (hybrid Euler discretization), after having set the parameters $\alpha, \lambda, \mu, \nu, \epsilon_0$ and T, consists of the following steps:

1) Set r_{max} (for example 100) and θ (usually 0.9) [1].

2) [*Fractional Power Series.*]
Compute the coefficients a_k ($k \in \mathbb{N}$) of the fractional power series $\psi(t) = \sum_{k \geq 1}^{\infty} a_k t^{k\alpha}$ up to r_{max}, using the recursive relation $(A_{\lambda,\mu,\nu})$ (see (2.8)).

3) [*Estimating The Convergence Radius*]
Knowing the coefficient $a_{r_{max}}$ allows us to use formula (3.4) to estimate the

---

[1]We set θ fixed and indipendent by n in our tests. Moreover, due to machines' limitations, we set r_{max} to be at most 110 in our experimentations.

convergence radius $\widehat{R}_\psi$.

4) [*Truncation*]
Truncate the coefficients up to a_{r_0}, with r_0 computed through the formula (3.5).

5) [*Compute $\bar{\psi}^n(t_k)$ for $k = 0, \cdots, n.$*]
For $n \in \mathbb{N}$ fixed, compute $\bar{\psi}^n(t_k)$ for $k = 0, \cdots, n$ in the following way: use the fractional power series for $k = 0, \cdots, k_0$, where $k_0 = \left\lfloor \frac{n\theta\widehat{R}_\psi}{T} \right\rfloor$. Use the recursive formula (3.8) for $k = k_0 + 1, \cdots, n$. Note that if $\theta\widehat{R}_\psi > T$ there is no need to use (3.8).

4.1.1   Real Results

We ran a test with the parameters (4.1), the precision set to $\epsilon_0 = 0.01$ and $T = \frac{1}{252}$. The first 4 steps are indipendent from n, so that the procedure in these steps is the same when computing $\bar{\psi}^n(t_k)$ for any n positive integer.

For step 1. We chose $r_{max} = 105$ and $\theta = 0.9$.

For step 2. the coefficients were computed up to the r_{max}-th coefficient. In this particular case, the modulo of the coefficients is increasing rapidly. In Table 4.1 are displayed some of the coefficients that we found numerically through the recursive relation $(A_{\lambda,\mu,\nu})$ (eq. (2.8)).

Table 4.1: coefficients of the fractional power series.

k	a_k	k	a_k	k	a_k
0	0	40	$-3.332270 \cdot 10^{77}$	95	$9.431333 \cdot 10^{180}$
1	$4.990864 \cdot 10^4$	41	$2.525245 \cdot 10^{79}$	96	$-7.183350 \cdot 10^{182}$
2	$-2.526168 \cdot 10^6$	42	$-1.914071 \cdot 10^{81}$	97	$5.471391 \cdot 10^{184}$
3	$1.711569 \cdot 10^8$	43	$1.451107 \cdot 10^{83}$	98	$-4.167590 \cdot 10^{186}$
4	$-1.175941 \cdot 10^{10}$	44	$-1.100332 \cdot 10^{85}$	99	$3.174595 \cdot 10^{188}$
5	$8.334470 \cdot 10^{11}$	45	$8.345019 \cdot 10^{86}$	100	$-2.418285 \cdot 10^{190}$
6	$-5.981382 \cdot 10^{13}$	46	$-6.330045 \cdot 10^{88}$	101	$1.842222 \cdot 10^{192}$
7	$4.336247 \cdot 10^{15}$	47	$4.802405 \cdot 10^{90}$	102	$-1.403434 \cdot 10^{194}$
8	$-3.165401 \cdot 10^{17}$	48	$- 3.644017 \cdot 10^{92}$	103	$1.069194 \cdot 10^{196}$
9	$2.323151 \cdot 10^{19}$	49	$2.765468 \cdot 10^{94}$	104	$-8.145842 \cdot 10^{197}$

The growth of the coefficients $\{a_k\}_{k\in\mathbb{N}}$ is exponential, confirmed by the plot of $f(k) = \log(|a_k|)$ in Figure 4.1.
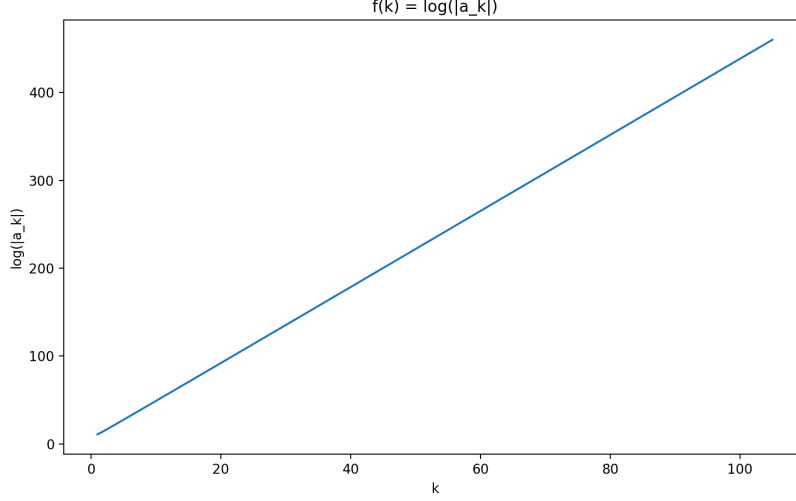
Figure 4.1: $f(k) = \log(|a_k|)$

For step 3. The estimated convergence radius is $\widehat{R}_\psi = 0.00109$ (the result is rounded), computed with the knowledge of $a_{r_{max}} = a_{105} = 6.21 \cdot 10^{199}$ and the formula (3.4):

$$\widehat{R}_\psi = |a'_{r_{max}}|^{-\frac{1}{\alpha r_{max}}} = |a'_{105}|^{-\frac{1}{\alpha \cdot 105}} = 0.00109,$$

where we used the formula (3.3) that gives us the relationship between the coefficients $\{a'_r\}_{r \in \mathbb{N}}$ and $\{a_r\}_{r \in \mathbb{N}}$.

Note that $\widehat{R}_\psi < \frac{1}{252} = T \approx 0.004$ so that

$$\theta \widehat{R}_\psi = 0.9 \widehat{R}_\psi < \frac{1}{252} = T.$$

Thus we will use the hybrid approach, as T does not belong to the domain of absolute convergence of the fractioanl power series: the fractional power series is used up to $\theta \widehat{R}_\psi$, after which the Euler scheme is applied in order to compute the values $\bar{\psi}^n(t_k)$, $k = 0, 1, \cdots, n$.

For step 4. Using formula (3.5) returns $r_0 = 102$. This means that in order to achieve an accuracy of $\epsilon_0 = 0.01$ with the fractional power series for $t \in [0, \theta \widehat{R}_\psi)$, it is enough to truncate up to a_{102}: thus we will consider the truncated series

$$\psi(t) = \sum_{k=0}^{102} a_k t^{k\alpha}.$$

For step 5. Fix n positive integer. In order to determine $\bar{\psi}^n(t)$ for any

$t \in [0, T]$, is necessary and sufficient to determine the values $\bar{\psi}^n(t_k)$ for $k = 1, \cdots, n$ (t_k and k_0 defined in (3.6)), since $\bar{\psi}^n$ is a piecewise step function. For $t_0, t_1, \cdots, t_{k_0}$ the fractional power series is used, i.e., we set

$$\bar{\psi}^n(t_k) = \sum_{n=0}^{102} a_n t_k^n, \quad k = 0, \cdots, k_0.$$

While for $t_{k_0+1}, \cdots, t_n$, the recurrent formula (3.8) based on the Euler scheme is used.

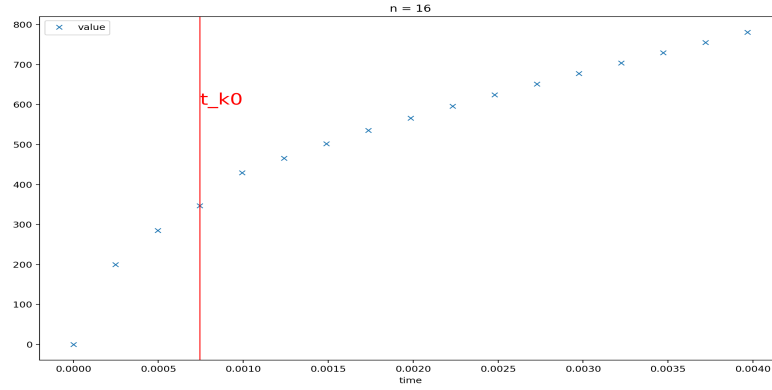Here we display some plots of $\bar{\psi}^n$ for different values of n ($n = 16, 64, 256$).
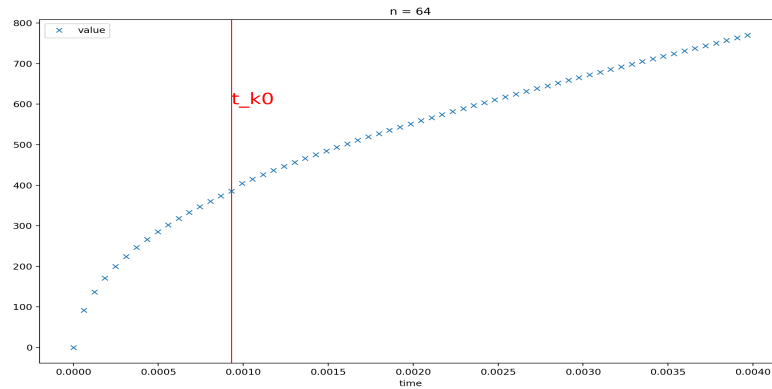

Figure 4.2: (a) $n = 16$
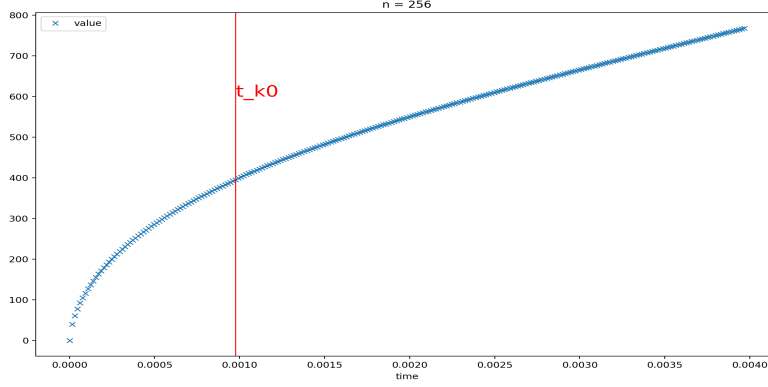

Figure 4.3: (b) $n = 64$

Figure 4.4: (c) $n = 256$

Each point represents the value of $\bar{\psi}^n(t_l)$ for $l \in \{1, 2, \cdots, n\}$. The red line is the value of t_{k_0}, which is the threshold that separates the methods we applied in order to compute the values of $\bar{\psi}^n(t_l)$, $l \in \{1, 2, \cdots, n\}$: the fractional power series is applied with the points on the left-side of the threshold t_{k_0} (i.e., for $t_0, t_1 \cdots, t_{k_0}$), and the Euler scheme with those on the right-side (i.e., for $t_{k_0+1}, \cdots, t_n$).

Notice that the transition from the evaluation of the power series to the Euler scheme is "smooth", even though we applied two different techniques. This suggests that the hybrid approach is consistent.

Moreover, notice that the shape has already formed for $n = 16$. Taking larger values of n does not change the shape, but only contributes to have a more "continuous" function.

Up to $n = 4096$, the computation times were quite reasonable, being under 1 minute the evaluation of each $\bar{\psi}^n$.

4.1.2 Computational Optimization and Observations

As suggested in [5], instead of solving the Riccati differential equation $\mathcal{E}^0_{\lambda,\mu,\nu}$ (eq. (11)), we can solve $\mathcal{E}^0_{1,\mu,\nu\lambda}$ if $\lambda \neq 0$, being faster from the computational point of view and equivalent to the original modulo scalar non-null multiplications. More precisely we have the following proposition:

Proposition 2. *Let ϕ be a solution to the Riccati differential equation $\mathcal{E}^0_{1,\mu,\nu\lambda}$ (eq. (11)) and $\lambda \neq 0$. Then $\psi := \frac{\phi}{\lambda}$ is a solution to $\mathcal{E}^0_{\lambda,\mu,\nu}$.*

Proof. Let ϕ be a solution to $\mathcal{E}^0_{1,\mu,\nu\lambda}$. Therefore it holds

$$D^\alpha \phi = \phi^2 + \mu\phi + \nu\lambda.$$

dividing both sides by λ (we assumed $\lambda \neq 0$) yields to

$$D^\alpha(\frac{\phi}{\lambda}) = \lambda \left(\frac{\phi}{\lambda}\right)^2 + \mu\frac{\phi}{\lambda} + \nu.$$

Defining $\psi := \frac{\phi}{\lambda}$ follows that ψ is a solution to $\mathcal{E}^0_{\lambda,\mu,\nu}$, as desired.   ∎

The optimal threshold factor $\theta = \theta(n)$ is suggested to be (see [5] for reference)

$$\theta(n) := \min\left(0.65 + 0.3\left(\frac{n-32}{4064}\right)^{0.25}, 0.925\right)$$

for $32 \leq n \leq 4096$. Notice that the function $\theta(n)$ defined above is increasing, reaching a maximum of 0.925. However, for values of $n \approx 2000$ we already have $\theta(n) \approx 0.9$, and preferably we would like to have greater values of n for a better accuracy. Moreover, for such values of n the computational cost is still very cheap for the machine (under one minute of computation for $\bar{\psi}^n$, $n \leq 4000$, in this particular test with my machine[2]). This is why in our experimentations we set $\theta = 0.9$ fixed independent by n.

Other things to add 4) Some comments on the time of execution with the simplified version (dividing both sides by λ)...

4.2   Computing c_1

In this section we continue the numerical tests from the previous section, i.e., same parameters (4.1) and $T = \frac{1}{252}$ with precision set to $\epsilon_0 = 0.005$. As discussed previously (Subsection 3.2.4 and Section 3.3), if we assume true the estimate (3.9), which we remind being

$$\bar{\psi}^n(T) - \psi(T) = \frac{c_1}{n} + o(n^{-1})$$

for some constant $c_1 \in \mathbb{R}$, then we can use the Richardson-Romberg extrapolation. Furthermore, the constant c_1 can be computed as described in Remark 6, i.e., as limit of the sequence $\{\bar{c}_1^n\}_{n\in\mathbb{N}}$, which we remind being defined as

$$\bar{c}_1^n := 2n\left(\bar{\psi}^n(T) - \bar{\psi}^{2n}(T)\right).$$

From the previous Section (Section 4.1) we already have the algorithm to compute $\bar{\psi}^n(T)$ for any n positive integer, so that we can easily find $\bar{c}_1^n$. The results that we got are in Table 4.2.

---

[2]A computer with 12 CPUs i7-8750H @ 2.20GHz.

Table 4.2: Values of $\bar{c}_1{}^n$ and computation times.

n	$\bar{c}_1{}^n$	computation time (seconds)	ratio of consecutive computation times
4	244.789055	0.005540	NaN
8	247.620217	0.005834	1.053153
16	236.228489	0.004871	0.834941
32	224.837873	0.005614	1.152562
64	215.948954	0.009873	1.758578
128	209.595284	0.018452	1.868924
256	205.598250	0.059347	3.216283
512	202.148404	0.221983	3.740396
1024	199.883079	0.862326	3.884654
2048	198.677258	3.469351	4.023247
4096	197.780231	14.281353	4.116433
8192	197.255466	57.106588	3.998682
16384	196.916654	227.248170	3.979369
32768	196.699728	926.553653	4.077277
65536	196.555097	3687.706343	3.980025
131072	196.510382	14858.320412	4.029150

It seems that the sequence $\{\bar{c}_1^n\}_{n\in\mathbb{N}}$ converges to some value, suggesting that the estimate (3.9) holds true. We take as reference limit the value

$$c_1^{ref} := \bar{c}_1^{n_{max}} = 196.510382,$$

where $n_{max} = 2^{17} = 131072$.

Now we will see some plots based on this data that strongly supports the validity of the two estimates (3.9) and (3.12), which we remind being, respectively,

$$\bar{\psi}^n(T) - \psi(T) = \frac{c_1}{n} + o(n^{-1})$$

for a constant $c_1 \in \mathbb{R}$ and

$$\bar{\psi}^n(T) - \psi(T) = \frac{c_1}{n} + \frac{c_2}{n^2} + o(n^{-2})$$

for some constants $c_1, c_2 \in \mathbb{R}$. We will refer to them as the RR estimates (first and second order respectively), since they allow us to perform the Richardson-Romberg extrapolation.

4.2.1 Plots and confirmation of the RR estimates

Figure 4.5 shows $\bar{c}_1{}^n$ in function of n (for numerical values see Table 4.2).
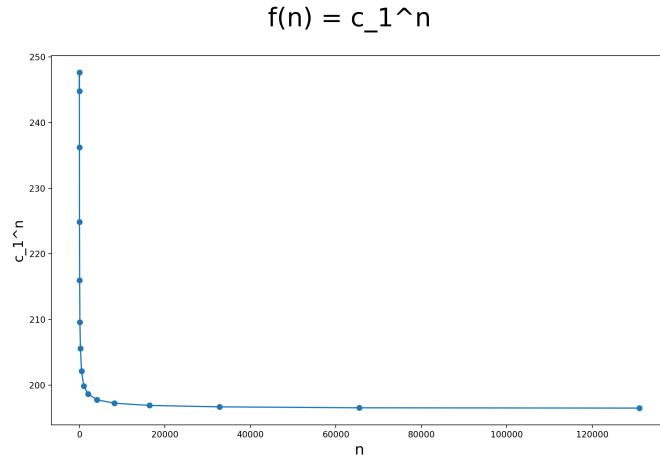
Figure 4.5: $f(n) = \bar{c}_1^n$

From the plot in Figure 4.5 it is more evident that the sequence $\{\bar{c}_1^n\}_{n\in\mathbb{N}}$ seems to converge. If the RR estimate (3.9) holds true, then a necessary condition is that

$$\lim_{n\to+\infty} \bar{c}_1^{\,n} \to c_1,$$

as shown in (3.10). However, this is not a sufficient condition for the RR estimate to hold true.

Now, the plot in Figure 4.6 is the $\log(\bar{c}_1^{\,n} - \bar{c}_1^{\,ref})$ in function of $\log(n)$
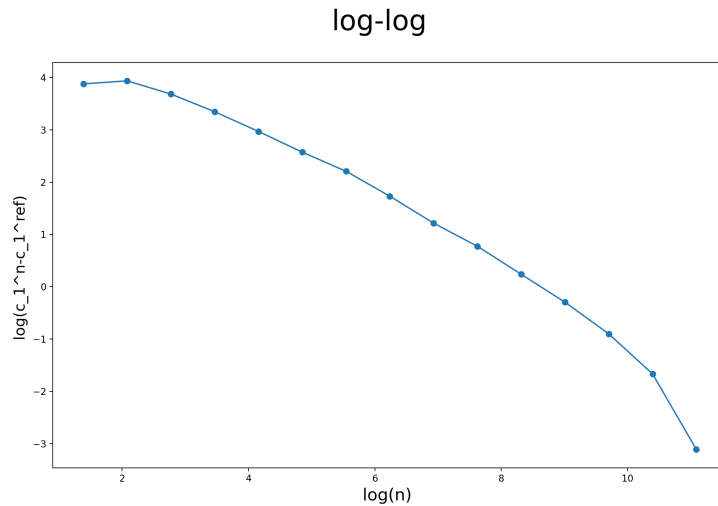

Figure 4.6: $\log(\bar{c}_1^{\,n} - \bar{c}_1^{\,ref})$ vs $\log(n)$

In this particular case, after applying a linear regression, we got that a coefficient of -0.68382593 is fitting the curve. However, if the second order RR estimate were to hold true:

$$\bar{\psi}^n(T) - \psi(T) = \frac{c_1}{n} + \frac{c_2}{n^2} + o(n^{-2}),$$

we would have that (considering $c_1 \approx c_1^{ref}$)

$$
\begin{aligned}
\bar{c_1}^n - c_1^{ref} &= 2n\left(\bar{\psi}^n(T) - \bar{\psi}^{2n}(T)\right) - c_1^{ref} \\
&= 2n\left(\frac{c_1}{n} + \frac{c_2}{n^2} - \frac{c_1}{2n} - \frac{c_2}{4n^2} + o(n^{-2})\right) - c_1^{ref} \\
&= 2n\left(\frac{c_1}{2n} + \frac{3c_2}{4n^2} + o(n^{-2})\right) - c_1^{ref} \\
&= c_1 + \frac{3c_2}{2n} + o(n^{-1}) - c_1^{ref} \\
&\approx \frac{3c_2}{2n},
\end{aligned}
\tag{4.2}
$$

which implies

$$\log(\bar{c_1}^n - c_1^{ref}) \approx \log(\frac{3c_2}{n}) = C - \log(n). \tag{4.3}$$

Letting $\log(n) = x$ and $\log(\bar{c_1}^n - c_1^{ref}) = y$, we have $y = -x + C$. Thus the plot above should be approximately linear with coefficient -1, while we obtained ≈ -0.68. This tells us that the second order RR estimate might not be true, but rather is of the form

$$\bar{\psi}^n(T) - \bar{\psi}(T) = \frac{c_1}{n} + \frac{c_2}{n^{2-\beta}} + o(n^{\beta-2}), \tag{4.4}$$

with $\beta \in (0,1)$ might depend on λ, μ, ν. Performing similar computations as in (4.2) yields to

$$\log(\bar{c_1}^n - c_1^{ref}) \approx C - (1-\beta)\log(n) \tag{4.5}$$

In our particular case it would be $(1-\beta) = -0.6838$, which means $\beta \approx -0.32$. However, in all of this, it is noted in [5] that the regression coefficient changes as we consider wider ranges of values for n. to write better

These observations suggest that the RR estimate of second order (eq. (3.12)) and the estimate in equation (4.4) do not hold true. However, all this does not imply that the double step RR extrapolation (described in Subsection 3.3.1 and equation (3.13)) is useless: we remind that $\left\{\bar{\psi}^n_{RR,3}\right\}_{n\in\mathbb{N}}$ does converge to ψ (as $n \to +\infty$), but the convergence rate (3.14) might not hold true since the second order RR estimate (3.12), from which it follows,

seems not to hold.

Below in Section 4.3 we will compare the computation times between the single step RR extrapolation method and the double step (i.e., computation times in seconds of $\left\{\bar{\psi}^n_{RR,2}\right\}_{n\in\mathbb{N}}$ and $\left\{\bar{\psi}^n_{RR,3}\right\}_{n\in\mathbb{N}}$, respectively, for some values of n) and the convergence rate in function of n.

4.2.2   Computational times for the sequence $\left\{\bar{c}^n_1\right\}_{n\in\mathbb{N}}$.

From Table 4.2 we observe that the computation time of $\bar{c}^n_1$ increases exponentilly with respect to n: if n doubles, the computational time of $\bar{c}^n_1$ quadruples.

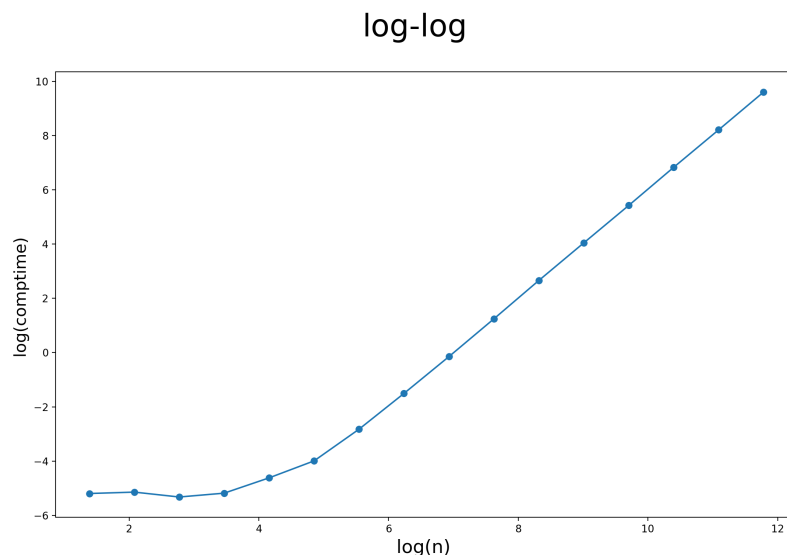In Figure 4.7 there is the plot of log(computation time of $\bar{c}^n_1$) vs log(n).

Figure 4.7: log(computation time of $\bar{c}^n_1$) vs log(n)

Applying a linear regression to the curve in Figure 4.7 yields a coefficient of 1.99993845 that fits the curve. We could have already expected it by looking at the results in Table 4.2 (for $n = 2^{15}$, computing $\bar{c}_1{}^n$ required about fifteen minutes, while for $n = 2^{16}$ it took an hour and for $n = 2^{17}$ it took four hours of computation).

4.3   Richardson-Romberg's extrapolations.

Now we compare the single step RR extrapolation (from which we obtain the sequence $\left\{\bar{\psi}^n_{RR,2}\right\}_{n\in\mathbb{N}}$) with the double step RR extrapolation (from

which we obtain the sequence $\left\{ \bar{\psi}_{RR,3}^{n} \right\}_{n\in\mathbb{N}}$) in terms of computation times[3] and convergence rate (as $n \to +\infty$).

We can observe from Table 4.3 and Figure 4.8 the values of $\bar{\psi}_{RR,2}^{n}(T)$ and $\bar{\psi}_{RR,3}^{n}(T)$ (computed through equations (3.13) and (3.11), respectively) and their relative computation times in seconds (the columns "comp. time RR2" and "comp. time RR3" of Table 4.3).

We can notice that $\bar{\psi}_{RR,3}^{n}(T)$ takes slightly more time than $\bar{\psi}_{RR,2}^{n}(T)$ to be computed. This could have been expected. Indeed, reminding equations (3.13) and (3.11), ... , it is clear that... This will surely be more visible with higher values of n. as we could have expected: we need to compute a more term: Riscrivi le formule.

However, $\bar{\psi}_{RR,3}^{n}(T)$ seems to converge faster than $\bar{\psi}_{RR,2}^{n}(T)$ (for $n \to +\infty$), as we can observe from Figure 4.8. in function of n.

So deciding whether to use one or the other is up to convenience: if we need fast convergence and we have no problems of powerful computers, then we can go for the RR3. If we need a quick computation and not a very precise estimate, we can go for RR2.

so, even if those RR estimate 2nd order does not hold true, the RR3 can be proven useful since it converges faster for n but it takes slightly more time to be comouted. It is to be evaluated from time to time....

We see it from the plot below. The tables also shows that the computational time for $RR3$ estimate is slightly higher than $RR, 2$, but it converges faster than $RR, 2$.

---

[3]In seconds. We remind that we use a computer with the following properties: 12 CPUs i7-8750H @ 2.20GHz. Even though the absolute times might change in different machines, we are more interested in ratios among different computation times.

Table 4.3: Richardson Romberg's estimates and computation times.

n	$\bar{\psi}^n_{RR,2}(T)$	$\bar{\psi}^n_{RR,3}(T)$	comp. time RR2 (s)	comp. time RR3 (s)
32	766.229560	766.466877	0.005526	0.010074
64	766.585516	766.704169	0.006187	0.007589
128	766.724406	766.770702	0.009566	0.010336
256	766.774044	766.790590	0.019738	0.019968
512	766.789657	766.794862	0.061665	0.065757
1024	766.796395	766.798641	0.227041	0.241486
2048	766.798607	766.799345	0.913140	0.979847
4096	766.799196	766.799392	3.645494	4.026486
8192	766.799415	766.799488	14.967328	15.561022
16384	766.799479	766.799501	60.779404	62.147462
32768	766.799500	766.799507	248.358794	308.513195
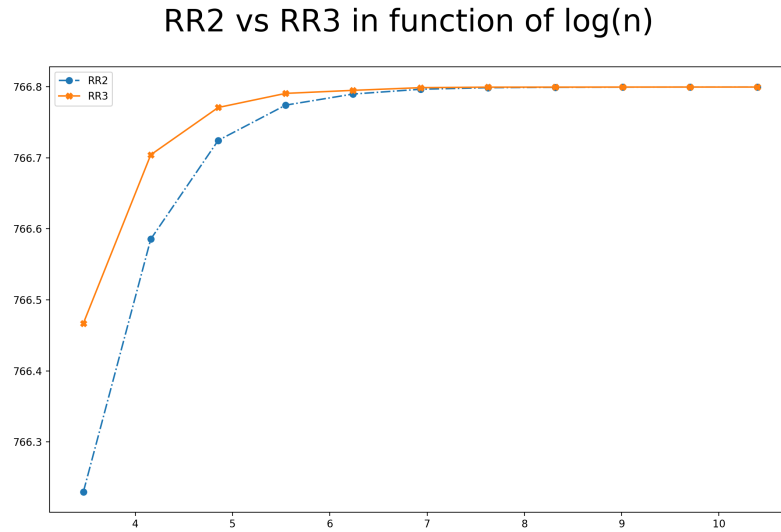
Figure 4.8: $RR2$ vs $RR3$ in function of $\log(n)$

4.4   Another Test with different parameters

Running another test with different parameters

$$\alpha = 0.64, \ \ \lambda = 0.2, \ \ \mu = -200, \ \ \nu = 200, \tag{4.6}$$

led to the following results. As for the coefficients we obtained the following:

Also in this case the growth of the coefficients looks exponential as we can see from the plot $f(k) = \log(|a_k|)$ (suggesting that it might exist some sort of relationship $a_k = m^k + \epsilon(k)$, for some function ϵ and constant m):

Table 4.4: Coefficients of the fractional power series.

k	a_k	k	a_k	k	a_k
0	0	40	$-1.687936 \cdot 10^{74}$	95	$1.354194 \cdot 10^{174}$
1	$2.225580 \cdot 10^{2}$	41	$1.102731 \cdot 10^{76}$	96	$-8.890316 \cdot 10^{175}$
2	$-3.469453 \cdot 10^{4}$	42	$-7.205620 \cdot 10^{77}$	97	$5.836737 \cdot 10^{177}$
3	$4.307108 \cdot 10^{6}$	43	$4.709280 \cdot 10^{79}$	98	$-3.832122 \cdot 10^{179}$
4	$-4.526010 \cdot 10^{8}$	44	$-3.078325 \cdot 10^{81}$	99	$2.516080 \cdot 10^{181}$
5	$4.174764 \cdot 10^{10}$	45	$2.012555 \cdot 10^{83}$	100	$-1.652058 \cdot 10^{183}$
6	$-3.465067 \cdot 10^{12}$	46	$-1.315989 \cdot 10^{85}$	101	$1.084779 \cdot 10^{185}$
7	$2.637354 \cdot 10^{14}$	47	$8.606478 \cdot 10^{86}$	102	$-7.123154 \cdot 10^{186}$
8	$-1.870412 \cdot 10^{16}$	48	$-5.629447 \cdot 10^{88}$	103	$4.677547 \cdot 10^{188}$
9	$1.254454 \cdot 10^{18}$	49	$3.682738 \cdot 10^{90}$	104	$-3.071697 \cdot 10^{190}$
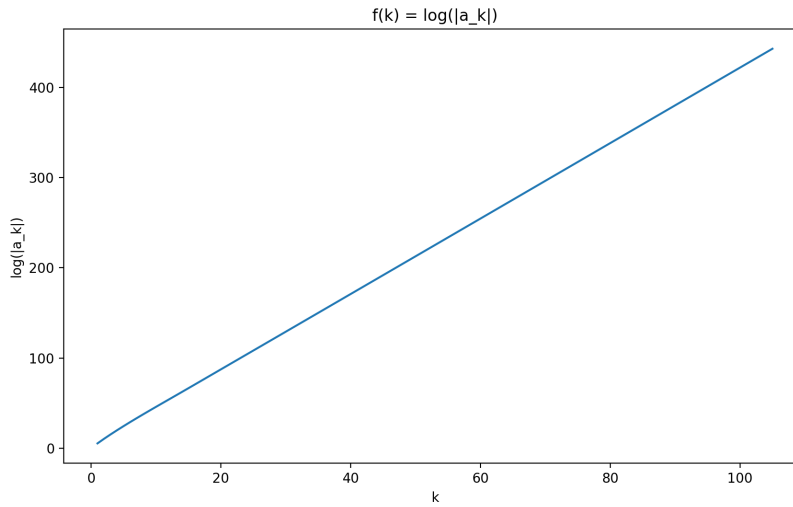
Figure 4.9: $f(k) = \log(|a_k|)$

Using the Euler Discretization scheme we computed some $\bar{\psi}^n$. Here are displayed $\bar{\psi}^n$ for $n = 16, 64, 256$. The shape of the curves are similar to those of the previous experimentation (see Figure **??**) with parameters as in (4.1).
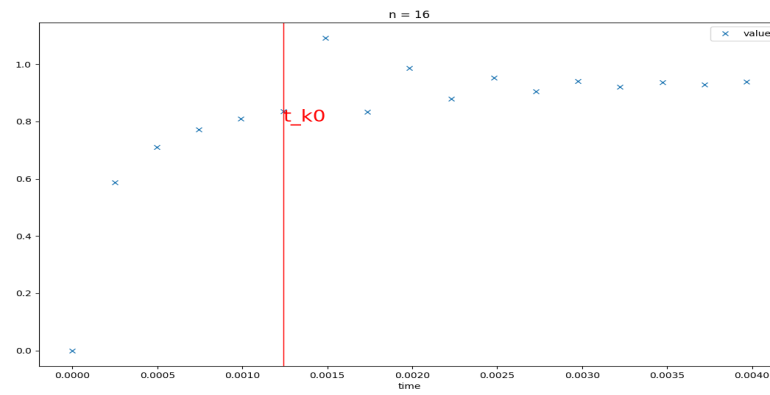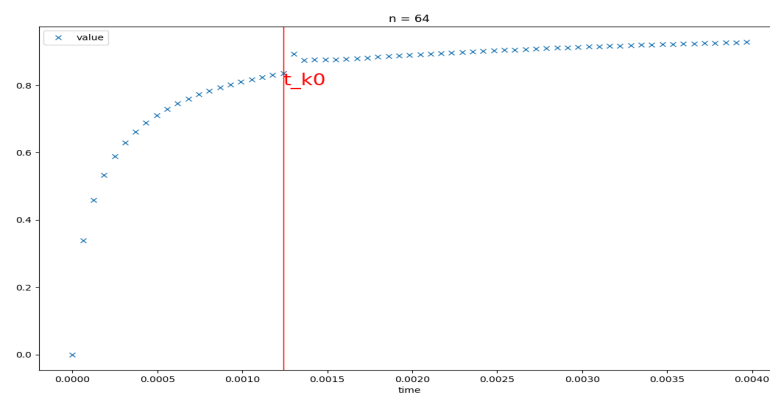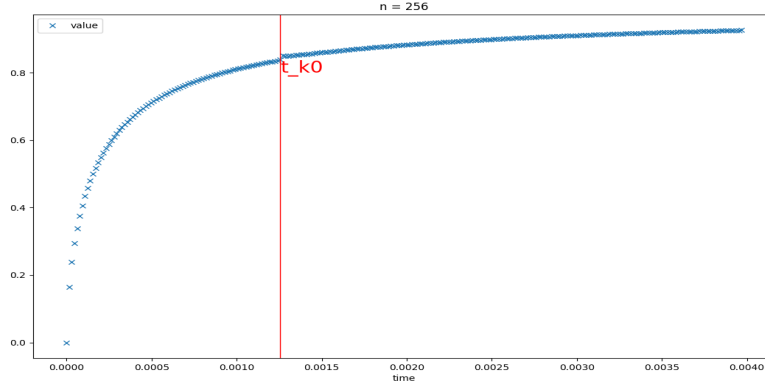
Figure 4.10: (a) $n = 16$


Figure 4.11: (a) $n = 64$

Figure 4.12: (a) $n = 256$

As for the sequence $\{\bar{c}_1{}^n\}_{n \in \mathbb{N}}$ (defined in Eq. 3.10), we obtained the following:

Table 4.5: Values of $\bar{c}_1{}^n$ and computation times.

n	$\bar{c}_1{}^n$	computation time (seconds)	ratio of consecutive computation times
4	45.992298	0.000978	NaN
8	-18.911034	0.001066	1.089956
16	0.262637	0.001241	1.164169
32	0.161077	0.002010	1.619789
64	0.151405	0.004920	2.447515
128	0.143325	0.016612	3.376496
256	0.140296	0.057853	3.482662
512	0.137850	0.225938	3.905420
1024	0.135780	0.904298	4.002411
2048	0.134314	3.672320	4.060962
4096	0.133632	14.989243	4.081682
8192	0.132789	60.255214	4.019897

The results are very similar to thos of the previous test: the computation times are comparable and the ratio of consecutive computation times also seems to converge to 4 as in the previous analysis. Furthermore, the sequence $\{\bar{c}_1{}^n\}_{n \in \mathbb{N}}$ seems to converge to a value around 0.13.
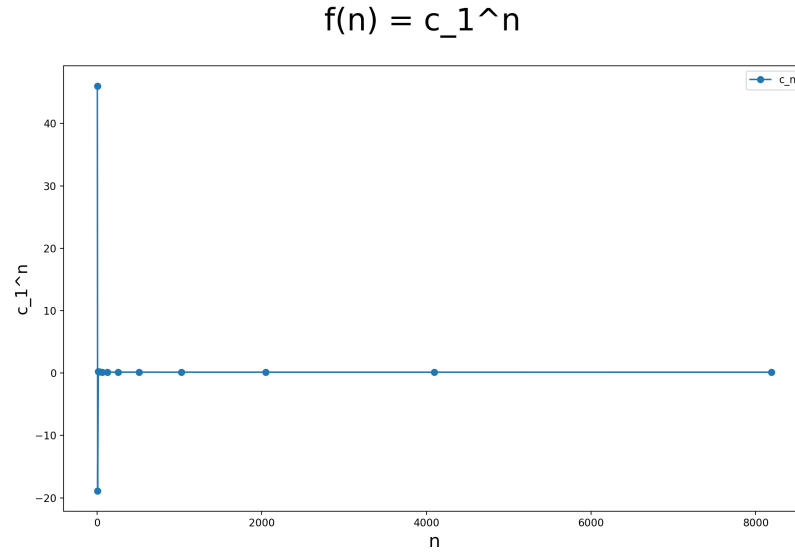
Figure 4.13: $f(n) = \bar{c}_1^n$

Finally, as it concerns the Richardson Romberg ...

Also here it seems that cns do converge (c_1^n ??).
And also the ratio of consecut compt times is around 4...

Table 4.6: Richardson Romberg's estimates and computation times.

n	RR2	RR3	comp. time RR2 (s)	comp. time RR3 (s)
32	0.922013	0.522561	0.002253	0.002648
64	0.925187	0.926245	0.003159	0.003967
128	0.925338	0.925388	0.005185	0.006413
256	0.925401	0.925422	0.016054	0.017432
512	0.925413	0.925417	0.061595	0.062513
1024	0.925417	0.925419	0.220778	0.232190
2048	0.925420	0.925420	0.852463	0.906958
4096	0.925420	0.925420	3.378545	3.681777
8192	0.925420	0.925420	13.629304	14.739946
16384	0.925421	0.925421	54.030256	58.376655
32768	0.925421	0.925421	215.273587	226.938969

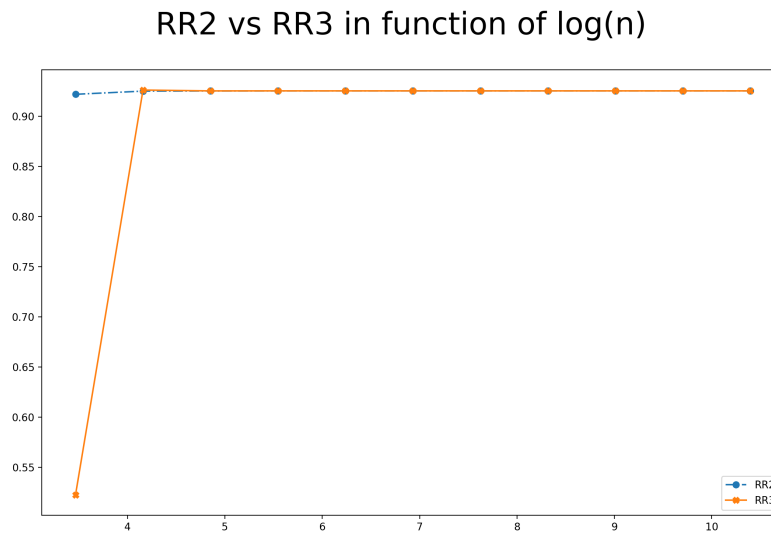Left to add RR2 vs RR3 in funct of logn.

Figure 4.14: $RR2$ vs $RR3$ in function of $\log(n)$

And just discuss that computational times are similar behaviour.

4.5 Additional Tests?

Un test è quello di rifare tutto ma applicando la semplificazione della moltiplicazione. Vedi sopra, invece di λ prendiamo $\lambda = 1$ e gli altri parametri riscalati.

Chapter 5

Other Plus final comments

What is left to do? precedentemente non abbiamo parlato dei tempi compitazionali di psi n. Per poi confrontare con machine learning forse. dove n può essere il numero di neuroni.

5.1 Forse aggiungerà la parte di machine learning se andrò in russia.

5.2 Commenti finali

5.2.1 Cose tralasciate

Cose che ho saltato. Salta la dimostrazione del teorema lungo sul raggio di convergenza. Poi salta anche la parte sul remainder term. Dove si stima di quanto si sbaglia troncando. Scrivi i risultati, ma senza dimostrazione. Inoltre, per gli altri metodi, non serve che metta come si ricava la tripletta. A noi interessa solo psi. Se scrivi troppo poco posso compensare parlando della discretizzazione di Eulero.

Bibliography

[1] Rogers, L.C.G. and Williams, D.: Diffusions, Markov Processes, and Martin- gales, Volume 1: Foundations. Cambridge University Press, 2000.

[2] Biagini F., Hu Yaozhong, Zhang Tusheng, Øksendal Bernt, *Stochastic Calculus for Fractional Brownian Motion and Applications*, Springer 2006

[3] El Euch, O. and Rosenbaum, *The characteristic function of rough Heston models.*. Mathe- matical Finance, 29(1):3–38, M. (2019)

[4] Samko, S., Kilbas, A., and Marichev. *Fractional integrals and derivatives. Theory and Applications*, Gordon and Breach, Yverdon, O. (1993).

[5] Callegaro G., Grasselli M., Pagès G. *Fast Hybrid Schemes for Fractional Riccati Equations (Rough is not so Tough)*, Mathematics of Operations Research, Vol. 46, 221-254, 2021

[6] Lalley P. Steven. *Introduction To Gaussian Processes.* https://galton.uchicago.edu/ lalley/Courses/386/GaussianProcesses.pdf

[7] Maslowski B., Nualart D. *Evolution equations driven by a fractional Brownian motion.* Journal of Functional Analysis, 277–305, 2003.

[8] Nourdin Ivan. *Selected aspects of fractional Brownian motion*, Bocconi Springer, 2004.

[9] Kallenberg O. *Foundations of modern probability.* Springer, 1997

[10] Rudin W. *Principles of Mathematical Analysis*, McGraw-Hill, 3rd edition, 1976

[11] Heston L. S., *A closed-form solution for options with stochastic volatility with applica- tions to bond and currency options.*, Review of Financial Studies. 327–343, 1993.

[12] Gatheral J., Jaisson T., Rosenbaum M. (2018). *Volatility is rough.* Quantitative Finance, 18(6):933– 949.

[13] *Cauchy formula for repeated integration*, Wikipedia.

[14] Nemes G., *New asymptotic expansion for the gamma function.* Archiv der Mathematik (Springer Basel) 95, 161-169 (2010)

[15] Pagès G. *Multi-step Richardson-Romberg extrapolation: remarks on variance control and complexity.* Monte Carlo Methods and Applications Journal, 13(1):37–70 (2007).

Appendix A

Python Code: Hybrid Euler Scheme

A.1   Computing $\left\{\bar{\psi}^n\right\}_{n\in\mathbb{N}}$.

Step 1.

```
alpha = 0.64
lambd = 0.045
mu = -64.938
nu = 44850

# error measures
epsilon = 0.01
theta = 0.9

r_max = 105
T = 1/252
```

Step 2.

```
import pandas as pd
import numpy as np
import math

def returns_all_the_first_r_max_coefficients_as_list_2():
    ''' Run this function. This returns the list of coefficients.
    Up to a_k where k = r_max. '''

    coefficients = [np.nan]*(r_max+1)

    a0 = 0
    a1 = nu/math.gamma(alpha+1)
```

```python
        coefficients [0] = a0
        coefficients [1] = a1

    def recursive_convol_coefficients(list_of_coefficients , k):
        ''' return a*_k^2  given the first k-1 a_m coefficients.
        k is the coefficient a^_k^2 to be returned '''
        if k==1:
            return 0
        else:
            sum = 0
            for l in range(1,k):
                a_l = list_of_coefficients [l]
                a_k_l = list_of_coefficients [k-l]
                sum += a_l*a_k_l
            return sum

    def recursive_coefficients(list_of_coefficients , n):
        ''' Given the convoluted coefficient a_k_star_quadro ,
        Given also n, the coefficient a_n to be returned.
        Note that n = k+1 !!!
        returns a_k'''

        k = n-1   #n-1 = k
        a_k_star_quadro = recursive_convol_coefficients(
                          list_of_coefficients , k)
        a_k = list_of_coefficients [k]
        a_n = (lambd*a_k_star_quadro + mu*a_k)*math.gamma(alpha*k+1)
              /math.gamma(alpha*k+alpha+1)

        return a_n

    for i in range(2, r_max+1):
        coefficients [i] = recursive_coefficients( coefficients , i)

    return coefficients

    coeff = returns_all_the_first_r_max_coefficients_as_list_2()
```

Step 3.

```python
a_r_max = coeff[-1]
a_primo_r_max = a_r_max*math.gamma(alpha*r_max+1)
              /math.gamma(alpha*r_max-alpha+1)
              /(alpha*r_max+1-alpha)
```

```
R_estimate = abs(a_primo_r_max)**(-1/(alpha*r_max))
```

Step 4.

```
r_0 = math.log(epsilon*(1-theta))/alpha/math.log(theta)-1
r_0 = int(np.round(r_0)+1)
```

Step 5.

```
def poly(lst, x):
    ''' Evaluate the polynomial with coefficients lst= [a0,a1,a2,...]
    in x.
    Pol: a0 + a1*x**alpha + a2*x**(2*alpha) + ....  '''
    n, tmp = 0, 0
    for a in lst:
        tmp = tmp + (a * (x**(n*alpha)))
        n += 1

    return tmp

def computing_psi_n(n):

    disc_times = [k*T/n for k in range(0,n+1)]

    k_0 = math.floor(R_estimate*theta*n/T)
    t_k_0 = disc_times[k_0]

    values_assumed_in_disc_times = [np.nan]*(n+1)

    ### Here We Evaluate The Truncated Series!
    for k in range(0,k_0+1):
        values_assumed_in_disc_times[k]=poly(coeff_truncated, disc_times[k])


    ### Here Instead We Use The Euler Scheme
    def compute_c_i(alpha, l):
        if l == 0:
            return 1
        else:
            return (l+1)**alpha - l**alpha


    for k in range(k_0+1, n+1):
        factor_1 = 1/math.gamma(alpha + 1)*(T/n)**alpha
        addend_2 = nu*k**alpha
```

```
        addend_3 = 0
        for l in range(1,k):
            psi_n_t_l = values_assumed_in_disc_times[l]
            addend_3 += compute_c_i(alpha, k-l-1)
                        *psi_n_t_l*(lambd*psi_n_t_l + mu)

        factor_2 = addend_2 + addend_3
        result = factor_1*factor_2
        values_assumed_in_disc_times[k] = result

    #return disc_times, values_assumed_in_disc_times
    return pd.DataFrame({"time": disc_times,
            "value": values_assumed_in_disc_times}), t_k_0
```

A.2   Computing $\{\bar{c_1}^n\}_{n\in\mathbb{N}}$.

Definition of the sequence $\{\bar{c_1}^n\}_{n\in\mathbb{N}}$.

```
def c_1(n):
    return (2*n*(computing_psi_n(n)[0].iloc[-1].value -
        computing_psi_n(2*n)[0].iloc[-1].value))
```

Computational times.

```
import time

df_ci_times = {}
df_ci_values = {}

for i in [2**k for k in range(2,14)]:
    start_time = time.time()
    df_ci_values[i] = c_1(i)
    df_ci_times[i] = time.time() - start_time

final = pd.DataFrame({"n": [key for key in df_ci_times],
    "c_n": [df_ci_values[key] for key in df_ci_values],
    "comput_time -sec -": [df_ci_times[key] for key in df_ci_times]})

final = final.set_index("n")

final['comput_time_rapport'] = (final['comput_time -sec -']/
    final['comput_time -sec -'].shift(1))

print(final)
```

A.3 Richardson-Romberg's estimates.

Definition of the Richardson-Romberg's estimates.

```
def richardson_romb_2(n) :
    if n%2 == 0:
        return (2*computing_psi_n(n)[0].iloc[-1].value -
            computing_psi_n(int(n/2))[0].iloc[-1].value)
    else:
        print('Error. Insert n even')


def richardson_romb_3(n):
    if n%4 == 0:
        addend_1 = 1/3*computing_psi_n(int(n/4))[0].iloc[-1].value
        addend_2 = -2*computing_psi_n(int(n/2))[0].iloc[-1].value
        addend_3 = 8/3*computing_psi_n(n)[0].iloc[-1].value
        return addend_1+addend_2+addend_3
    else:
        print('error. Insert n multiple of 4')
```

Computational times.

```
rr2 = {}
compt_time_2 = {}
rr3 = {}
compt_time_3 = {}

import time

for n in [2**k for k in range(5,16)]:
    start_time_2 = time.time()
    rr2[n] = richardson_romb_2(n)
    compt_time_2[n] = time.time()-start_time_2

    start_time_3 = time.time()
    rr3[n] = richardson_romb_3(n)
    compt_time_3[n] = time.time()-start_time_3

fin_extr = pd.DataFrame({"n": [key for key in rr2],
    "rr2": [rr2[key] for key in rr2],
    "rr3": [rr3[key] for key in rr3],
    "comp2" : [compt_time_2[key] for key in rr2],
    "comp3": [compt_time_3[key] for key in rr2]})

print(fin_extr)
```

Appendix B

Python Code: Machine Learning Parts

B.1 First Neural Networks

B.2 Others